

Aus der Klinik für Kinder-Onkologie, -Hämatologie  
und klinische Immunologie der Heinrich-Heine-Universität -  
Direktor: Prof. Dr. Arndt Borkhardt

**Proteasome inhibitors emerging as new therapy options for  
*ALK*-mutated neuroblastoma**

Dissertation

zur Erlangung des Grades eines Doktors der Medizin  
der Medizinischen Fakultät der  
Heinrich-Heine-Universität Düsseldorf

vorgelegt von  
**Johanna Katharina Jacobs**

Düsseldorf, Januar 2024

Als Inauguraldissertation gedruckt mit der Genehmigung  
der Medizinischen Fakultät der  
Heinrich-Heine-Universität Düsseldorf

gez.:

Dekan: Prof. Dr. med. Nikolaj Klöcker

Erstgutachter: Prof. Dr. med. Guido Reifenberger

Zweitgutachter PD Dr. med. Sujal Ghosh

## Zusammenfassung

Das Neuroblastom (NB) ist ein bösartiger Tumor des peripheren sympathischen Nervensystems und der häufigste extrakranielle solide Tumor bei Kindern. Bei Hochrisikopatienten liegt die 5-Jahres-Überlebensrate mit den bestehenden multimodalen Therapieschemata (Chemotherapie, Resektion, Strahlentherapie) trotz intensiver Forschung in den letzten Jahren bei unter 50%. Neue Therapieoptionen sind deswegen notwendig. Eine Keimbahnmutation im Proto-onkogen *Anaplastische Lymphomkinase (ALK)* ist die häufigste Ursache für familiär-bedingte Neuroblastome. Ein internes Hochdurchsatz-Screening von verschiedenen Medikamenten zeigte eine höhere Empfindlichkeit von *ALK*-mutierten (mut) NB-Zelllinien gegenüber dem Proteasom-Inhibitor Ixazomib. Daher wurde in dieser Arbeit Ixazomib als zusätzliche Therapieoption für *ALK*-mut NB geprüft.

Das Ziel der Arbeit war es, zu untersuchen, ob der neue Proteasom-Inhibitor Ixazomib eine signifikant bessere Wirksamkeit in *ALK*-mut NB-Zelllinien im Gegensatz zu *ALK*-wildtyp (wt) NB-Zelllinien aufweist. Dafür wurden sechs verschiedene humane NB-Zelllinien verwendet: Kelly, SH-SY5Y und CLBGA als *ALK*-mut NB-Zelllinien sowie IMR 32, SK-N-FI und NBL-S als *ALK*-wt Zelllinien. Um den Effekt von Ixazomib auf *ALK*-mut und *ALK*-wt Zellen zu untersuchen, wurden verschiedene Assays zur Quantifizierung der Zellviabilität und -proliferation, Apoptoseaktivität und DNA-Schädigung durchgeführt. Um mögliche molekularbiologische Mechanismen von Ixazomib nachzuweisen, wurden *realtime*-PCR und Western Blot Analysen speziell zur Bestimmung der NF- $\kappa$ B-Expression durchgeführt, da bisherige Studienergebnisse nahelegen, dass NF- $\kappa$ B in den Wirkmechanismus von Proteasom-Inhibitoren involviert ist.

Die Behandlung mit Ixazomib führte zu einer reduzierten Zellviabilität, hemmte die Zellproliferation, führte zu vermehrten Doppelstrangbrüchen und erhöhte die Apoptoseaktivität in *ALK*-mut NB-Zelllinien. Weder in *ALK*-wt noch in *ALK*-mut NB-Zellen wurde eine signifikante Ixazomib-induzierte Veränderung der NF- $\kappa$ B-Expression beobachtet.

Die Ergebnisse in dieser Arbeit deuten darauf hin, dass die Behandlung mit Ixazomib zu einer signifikanten Induktion von Zelltod in *ALK*-mut NB-Zelllinien führt. Daher könnte dieser relativ neue Proteasom-Inhibitor als zusätzliche Behandlungsoption für Patienten mit einem NB, das eine *ALK*-Mutation aufweist, dienen.

## Summary

Neuroblastoma (NB) is a malignant tumor of the peripheral sympathetic nervous system and the most common extracranial malignant solid tumor in children. For high-risk patients, the 5-year survival rate is less than 50% with existing multimodal therapy regimens (chemotherapy, resection, radiotherapy). Thus, new therapy options are required. The *anaplastic lymphoma kinase (ALK)* gene mutation is considered a proto-oncogene and is the most common inheritable mutation in NB. In-house high-throughput drug screening revealed higher sensitivity of *ALK* mutated (mut) NB cell lines towards ixazomib. Therefore, the proteasome inhibitor ixazomib was evaluated as an additional therapeutic strategy for *ALK* mut NB.

The aim of this work was to determine whether the novel proteasome inhibitor ixazomib has a better efficacy in *ALK* mut NB cell lines in comparison to *ALK* wildtype (wt) NB cell lines. For this purpose, six commercially available human NB cell lines were investigated: Kelly, SH-SY5Y, CLBGA as *ALK* mut NB cell lines and IMR 32, SK-N-FI, NBL-S as *ALK* wt cell lines. To evaluate the effects of ixazomib treatment on *ALK* mut and *ALK* wt cells, various assays were performed to quantify cell viability and proliferation, apoptotic activity, and DNA damage. To assess possible molecular mechanisms of ixazomib, real-time PCR and Western blot analyses were performed specifically for detection of NF- $\kappa$ B expression, as previous study results suggested that NF- $\kappa$ B is involved in the mechanism of action of proteasome inhibitors.

Ixazomib treatment led to reduced cell viability, inhibited cell proliferation and increased apoptosis. Furthermore, *ALK* mut cell lines showed increased DNA damage after ixazomib treatment. No significant ixazomib-induced alteration in NF- $\kappa$ B expression was observed, neither in *ALK* wt nor in *ALK* mut NB cells.

In conclusion, the results summarized in this thesis indicate that ixazomib treatment leads to significant induction of the cell death machinery in *ALK* mut NB cell lines. Therefore, this relatively new proteasome inhibitor may serve as additional treatment option in patients with NB carrying an *ALK* mutation.

## Abbreviations

$\mu$	Micro
<sup>123</sup> I	Iodine-123
<sup>131</sup> I	Iodine-131
<b>ACTB</b>	Actin Beta
<b>ALK</b>	Anaplastic lymphoma kinase
<b>ATRX</b>	Alpha thalassemia/mental retardation syndrome X-linked
<b>BSA</b>	Bovine serum albumin
<b>cDNA</b>	Complementary DNA
<b>CT</b>	Computed tomography
<b>DAPI</b>	4',6-diamidino-2-phenylindole
<b>ddH<sub>2</sub>O</b>	Double distilled water
<b>DMSO</b>	Dimethylsulfoxide
<b>DNA</b>	Deoxyribonucleic acid
<b>dNTP</b>	Deoxyribonucleotide triphosphate
<b>DTT</b>	Dithiothreitol
<b>EDTA</b>	Ethylenediaminetetraacetic acid
<b>EdU</b>	5-ethynyl-2'-deoxyuridine
<b>EtOH</b>	Ethanol
<b>FBS</b>	Fetal bovine serum
<b>FITC</b>	Fluorescein isothiocyanate
<b>FOS</b>	Fos Proto-Oncogene, AP-1 Transcription Factor Subunit
<b>g</b>	Gramm
<b>GAPDH</b>	Glyceraldehyde 3-phosphate dehydrogenase
<b>GPOH</b>	Gesellschaft für pädiatrische Onkologie und Hämatologie
<b>GUSB</b>	Glucuronidase Beta
<b>Gy</b>	Gray
<b>h</b>	Hour
<b>HRP</b>	Horseradish peroxidase
<b>IC<sub>50</sub></b>	Half maximal inhibitory concentration
<b>IDRF</b>	Image Defined Risk Factors
<b>IKBKB</b>	Inhibitor Of Nuclear Factor Kappa B Kinase Subunit Beta
<b>IKK</b>	I $\kappa$ B kinase
<b>IMDM</b>	Iscove's Modified Dulbecco Medium
<b>INRG</b>	International Neuroblastoma Risk Group
<b>I<math>\kappa</math>B<math>\alpha</math></b>	Nuclear factor of kappa light polypeptide gene enhancer in B-cells inhibitor, alpha
<b>IPA</b>	Ingenuity pathway analysis
<b>JNK</b>	c-Jun NH <sub>2</sub> terminal kinase
<b>kDa</b>	Kilo Dalton
<b>l</b>	Liter
<b>M</b>	Mole
<b>m</b>	Milli
<b>mAb</b>	Monoclonal antibodies
<b>MIBG</b>	Meta-Iodobenzylguanidine
<b>min</b>	Minute
<b>M-MLV RT</b>	Moloney Murine Leukemia Virus Reverse Transcriptase
<b>MRI</b>	Magnetic resonance imaging
<b>mRNA</b>	Messenger ribonucleic acid

<b>mut</b>	Mutated
<b>MYCN</b>	MYCN proto-oncogene, bHLH transcription factor
<b>n</b>	Nano
<b>N/A</b>	Not available
<b>NB</b>	Neuroblastoma
<b>NF-κB</b>	Nuclear Factor Kappa B
<b>NF-κB1</b>	Nuclear Factor Kappa B Subunit 1
<b>NF-κB2</b>	Nuclear Factor Kappa B Subunit 2
<b>NPM</b>	Nucleophosmin
<b>NRAS</b>	NRAS Proto-Oncogene, GTPase
<b>NSCLC</b>	Non-small-cell lung cancer
<b>NSE</b>	Neuron specific enolase
<b>PBS</b>	Phosphate buffered saline
<b>PBS-T</b>	Phosphate-buffered saline with Tween
<b>PCR</b>	Polymerase chain reaction
<b>PHOX2B</b>	Paired-like homeobox 2b
<b>PI</b>	Propidium iodide
<b>PPIA</b>	Peptidylprolyl Isomerase A
<b>PTPN11</b>	Protein tyrosine phosphatase non-receptor type 11
<b>RELA</b>	RELA Proto-Oncogene, NF-κB Subunit
<b>RELB</b>	RELB Proto-Oncogene, NF-κB Subunit
<b>RIPA</b>	Radioimmunoprecipitation assay
<b>RNA</b>	Ribonucleic acid
<b>RPL13</b>	Ribosomal Protein L13
<b>RSC</b>	Rapid Sample Concentrator
<b>RT</b>	Room temperature
<b>SDS</b>	Sodium dodecyl sulfate
<b>SDS-PAGE</b>	Sodium dodecyl sulfate polyacrylamide gel electrophoresis
<b>SEM</b>	Standard error of mean
<b>TBS-T</b>	Tris-buffered saline with Tween
<b>TERT</b>	Telomerase reverse transcriptase
<b>TGM2</b>	Transglutaminase 2
<b>WHO</b>	World Health Organization
<b>wt</b>	Wildtype
<b>xg</b>	Times gravity

## Table of contents

1	Introduction.....	1
1.1	Neuroblastoma.....	1
1.1.1	Clinical presentation .....	1
1.1.2	Diagnostics.....	2
1.1.3	Risk stratification .....	2
1.1.4	Genetic analysis .....	3
1.1.5	Treatment options.....	4
1.2	Anaplastic lymphoma kinase.....	5
1.3	Proteasome inhibitors as therapy option .....	6
1.4	Aim of the thesis .....	8
2	Materials and Methods .....	10
2.1	Materials .....	10
2.1.1	Cell lines.....	10
2.1.2	Media and supplements .....	10
2.1.3	Buffers .....	11
2.1.4	Chemicals.....	11
2.1.5	Specific reagents and other materials .....	12
2.1.6	Primers .....	13
2.1.7	Enzymes.....	14
2.1.8	Antibodies.....	15
2.1.9	Commercially available kits .....	16
2.1.10	Other consumables .....	16
2.1.11	Devices .....	17
2.1.12	Software .....	19
2.2	Methods .....	20
2.2.1	Cell cultivation .....	20
2.2.2	Cell cryopreservation.....	20

2.2.3	Dilution series .....	20
2.2.4	Treatment with ixazomib.....	21
2.2.5	Cell proliferation.....	21
2.2.6	Crystal violet staining.....	22
2.2.7	Cell viability .....	22
2.2.8	Annexin V .....	22
2.2.9	Caspase 3/7 .....	22
2.2.10	DNA damage.....	23
2.2.11	Ingenuity pathway analysis .....	23
2.2.12	RNA extraction, cDNA synthesis, quantitative real-time PCR ...	24
2.2.13	Cell lysis, protein extraction and Western blot.....	25
2.2.14	Statistical analyses.....	26
3	Results.....	27
3.1	Treatment with ixazomib reduces the oncophenotype in <i>ALK</i> mutated neuroblastoma cells .....	27
3.1.1	Decreased cell viability in <i>ALK</i> mutated neuroblastoma cell lines after ixazomib treatment .....	28
3.1.2	Increased apoptosis in <i>ALK</i> mutated neuroblastoma cell lines after ixazomib treatment compared to <i>ALK</i> wildtype cell lines .....	29
3.1.3	<i>ALK</i> mutated neuroblastoma cell lines show more DNA damage upon ixazomib treatment compared to <i>ALK</i> wildtype cell lines .....	32
3.2	Possible ixazomib targets in <i>ALK</i> mutated neuroblastoma cell lines...	34
3.3	Validation of NF- $\kappa$ B involvement in the molecular mechanisms of ixazomib in the treatment of <i>ALK</i> mutated neuroblastoma on mRNA and protein levels	35
4	Discussion .....	37
4.1	Importance of novel therapeutic strategies for neuroblastoma.....	37
4.2	Additional mutations influencing the effect of ixazomib in neuroblastoma cell lines .....	38

4.3	NF- $\kappa$ B as possible target for ixazomib in neuroblastoma cell lines .....	39
4.4	Development of resistance of <i>ALK</i> mutated neuroblastomas to <i>ALK</i> inhibitors .....	41
4.5	Limitations .....	41
4.6	Conclusion and Outlook .....	42
5	References .....	43

# **1 Introduction**

## **1.1 Neuroblastoma**

Neuroblastoma (NB) is a malignant embryonic tumor that arises from immature cells of the sympathetic nervous system. It is the most common extracranial malignant solid tumor in childhood as well as the the most common cancer diagnosed in the first year of life [1-3]. Interestingly, there are NBs that regress completely spontaneously, mostly in infants [4]. In older patients, NBs can be very resistant against different kinds of therapy [5]. They are classified in low-, intermediate- and high-risk groups, depending on clinical presentation, imaging and genetics [6]. Neuroblastomas have variable organic and clinical manifestations [1] and account for about 5.5% of all cancers in childhood and adolescence [7]. According to the German Childhood Cancer Registry (Mainz), approximately 120 children and adolescents under the age of 18 are newly diagnosed with NB in Germany each year.

Since NBs are embryonic tumors, they occur primarily in early childhood: 90% of patients are younger than five years old. The average age at diagnosis is two years [2]. Most affected, approximately 46% of patients, are newborns and infants in the first year of life. Boys have a slightly higher incidence rate than girls (ratio 1.4 : 1) [7]. However, NB can also occur in older children, adolescents and, in some cases, even in adults [8]. The overall five-year survival rate for patients with NB is higher than 80% [3].

### **1.1.1 Clinical presentation**

Since NB is an embryonal tumor of the sympathetic nerve tissue, it can occur anywhere along the sympathetic nervous system. Most common manifestations are the adrenal gland, the paravertebral area, abdomen, chest, neck and pelvis [1]. At the time of diagnosis, metastases are already observed in approximately 50% of patients, typically in bone marrow, bones and lymph nodes. The symptoms are dependent on the localization of the primary tumor and the presence of metastases or paraneoplastic syndromes [9]. Swelling is common and caused by the tumor or metastases. With manifestations in the neck or chest, the tumor may cause Horner's syndrome (ptosis, miosis and anhidrosis). If the tumor is located in paravertebral areas, it may lead to paralysis caused by

peripheral nerve or spinal cord compression. Especially when metastasized, NB patients can have general symptoms like fatigue, fever and pain of the bones. [1, 10].

### **1.1.2 Diagnostics**

When NB is suspected, the concentration of catecholamine metabolites such as homovanillic acid and vanillylmandelic acid can be determined in the urine [11]. Furthermore, the tumor marker neuron specific enolase (NSE) can be measured from blood samples. Elevated NSE values must be critically evaluated in conjunction with the other findings [12]. For imaging diagnostics, a chest X-ray as well as an ultrasound of neck, abdomen and pelvis are performed, followed by computed tomography (CT) or magnetic resonance imaging (MRI) of the tumor region [10]. The advantages of MRI are no radiation exposure and the visualization of paraspinal tumor tissue at relatively high spatial resolution, which could eventually lead to spinal cord compression [9]. The goal of the initial cross-sectional imaging is to completely assess the extent of the primary tumor and metastases and to determine the International Neuroblastoma Risk Group (INRG) stage based on Image Defined Risk Factors (IDRF) [13]. Another highly specific method for the confirmation of suspected neuroectodermally derived tumors such as NB or the resulting metastatic disease is iodine-123-meta-iodobenzylguanidine ( $^{123}\text{I}$ -MIBG) scintigraphy [14].

Combined with chemical profiling and imaging characteristics, histologic confirmation is required to secure the diagnosis. Usually, a biopsy of the primary tumor is obtained. In case of metastases, bone marrow aspiration is also required. [9, 15].

### **1.1.3 Risk stratification**

Approaches for risk stratification vary throughout the world. To serve a more consistent approach, the INRG classification system was established. In a cohort of 8,800 children diagnosed with NB, 13 prognostic factors were analyzed regarding the event-free survival. Factors which belong to the most highly statistically significant and clinically relevant factors include stage, age, histologic category, grade of tumor differentiation, the status of the *MYCN proto-oncogene*, *bHLH transcription factor (MYCN)* oncogene, chromosome 11q and 1p status,

and DNA ploidy. [16]. For the classification system the age of 18 months was selected as cut-off. Based on the INRG classification system patients are now classified as very low-risk, low risk, intermediate-risk or high-risk, depending on clinical criteria and tumor imaging. The 5-year event-free survival rate is more than 85% for very low-risk NB, > 75% to ≤ 85% for low-risk NB, ≥ 50% to ≤ 75% for intermediate-risk NB and less than 50% for high-risk NB [16].

#### 1.1.4 Genetic analysis

To determine the risk and prognosis of NB, genetic factors are important in addition to clinical and imaging criteria. They include amplifications of *MYCN*, the ploidy status, chromosomal deletions and gene mutations, and they correlate with clinical outcome [6, 15]. For more than two decades, *MYCN* status is accepted for therapy stratification [17]. It is one of the most important prognostic factors and is associated with rapid tumor progression and poor prognosis [2, 18]. Ploidy is a general term that describes the number of complete sets of chromosomes in a cell, with a normal (diploid) cell having two complete sets of chromosomes, i.e., 1 maternal and 1 paternal chromosome set. A normal cell has a DNA index of 1. In children younger than 18 months, hyperdiploid (DNA index > 1) NBs are associated with a more favorable outcome [6, 15]. Aberrations at the chromosomal level that are associated with poor outcome include deletion of 1p36 and 11q as well as unbalanced gain of chromosome arm 17q [19, 20]. Genes that commonly show somatic mutations in association with NB include *anaplastic lymphoma kinase gene (ALK)*, *protein tyrosine phosphatase non-receptor type 11 gene (PTPN11)*, *alpha thalassemia/mental retardation syndrome X-linked gene (ATRX)*, *MYCN* and *NRAS Proto-Oncogene, GTPase (NRAS)* with *ALK* being the most common mutated gene [21]. Germline mutations in *ALK* are the second most common driver mutations of NB, found in 8-10% of NB patients [22-24]. These also explain the majority of hereditary NBs, which occur in 1-2% of the NB cases [22, 25]. Furthermore, *ALK* mutations are suggested to drive disease relapse [2]. For patients with associated disorders of the autonomic nervous system such as Hirschsprung's disease, *paired-like homeobox 2b (PHOX2B)* gene mutations are most likely involved in the initiation of tumorigenesis [26]. Currently, targeted or genome-wide sequencing (e.g. to identify *ALK* alterations or mutations) is almost always performed for NB diagnosis whenever possible [2].

### **1.1.5 Treatment options**

#### **Low-risk**

At the time of diagnosis, surgery is required to obtain tumor tissue for histology and molecular analysis. It can be performed either conventionally or, if possible, also minimally invasive. If IDRF are missing at the time point of surgery and the tumor is not predicted to be high-risk, the tumor can also be resected at once. However, extensive operations are not advised due to the high rate of spontaneous regression of tumors at this stage. Chemotherapy is only necessary if the tumor causes any clinical symptoms. [10]. Due to the potential long-term side effects, radiotherapy and <sup>131</sup>I-MIBG therapy are not part of the regular therapy for patients with low-risk NB [8].

#### **Intermediate-risk**

As for the low-risk group, surgery is required to obtain tumor tissue for histology and molecular analysis at the time of diagnosis. Complete resection at this time is, as for the low-risk group, only justified if it proves to be unproblematic intraoperatively and can be performed without any additional damage to the surrounding tissue. Otherwise, induction chemotherapy is given. The overall goal is a complete surgical removal of the tumor, followed by maintenance chemotherapy. If the tumor is not resectable or if there is residual viable tumor, a consolidating radiotherapy with a total dose of 36-40 Gray (Gy) will be performed. [8].

#### **High-risk**

In high-risk patients, the primary aim of the initial surgery is the extraction of tumor tissue for histology and molecular analysis. An initial complete resection of the tumor is only performed if image-defined risk factors are not present and, under the given circumstances, that the surgery is low risk and appears to be unproblematic. Otherwise, the primary resection should only take place after 2-4 neoadjuvant chemotherapy cycles. Since there is only a limited number of available cytotoxic drugs effective for high-risk NB [8], another therapeutic option is myeloablative therapy and autologous hematopoietic cell rescue. In a long-term study, this showed significantly better five-year event-free survival and overall survival compared to conventional non-myeloablative chemotherapy [27]. Another therapy option against refractory or relapsed NB is <sup>131</sup>I-MIBG therapy [8].

As a tumor derived from the neural crest, NBs typically express norepinephrine transporters, which can be used for imaging-based diagnosis as well as therapy in a theranostics setting. The transporters provide intracellular uptake and retention of MIBG in approximately 90% of affected patients [28]. When MIBG is radiolabelled with  $^{131}\text{I}$ , it provides tumor-specific radiation and is used for targeted therapy as well as for diagnostic purposes when loaded with  $^{123}\text{I}$  [29]. To minimize the side effects of the myelosuppressive effects of radiation, therapy at high doses of  $^{131}\text{I}$ -MIBG is supported by autologous peripheral blood stem cell transplantation [29]. If unresectable vital residual tumor should be present after surgery and induction therapy, the current strategy of the *Gesellschaft für pädiatrische Onkologie und Hämatologie* (GPOH) recommends external beam radiotherapy following myeloablative chemotherapy and autologous stem cell transplantation. For external beam radiotherapy, a total dose of 36-40 Gy should be reached. As maintenance therapy, the combination of isotretinoin, immunotherapy with anti-GD2 antibodies and exogenous cytokines has improved outcomes in high-risk patients [2]. Late-onset side effects occur very frequently in surviving patients after more than five years from diagnosis and include secondary malignancies, learning difficulties and reproductive health concerns for high-risk patients [2]. It is always important that the possible long-term side effects of the therapy are balanced with its potential therapeutic benefits in a risk/benefit calculation [8].

Since the majority of patients with NB are treated within clinical trials, other study-specific therapies and stratification algorithms are often applied [10].

Regular follow-up visits are recommended for all patient groups so disease relapse or late developing toxicities from treatment can be detected at an early stage [8].

## **1.2 Anaplastic lymphoma kinase**

*ALK* is a receptor tyrosine kinase that is mainly expressed in the neural system [30, 31]. It was first described in 1994 as a fusion gene between *nucleophosmin* (*NPM*) and *ALK* in the t(2;5) chromosomal translocation associated with anaplastic large-cell T-cell non-Hodgkin lymphoma [32]. *ALK* is located on chromosome band 2p23, expressed in the small intestine, testis and brain, and has a close similarity to the insulin receptor subfamily of kinases [32]. It is

predicted that *ALK* is involved in the development of the brain and the nervous system [31]. In NB, the oncogenic effect of *ALK* is not due to the formation of fusion proteins but is caused by *ALK* amplifications and *ALK* driver mutations [30]. Gene amplification results in increased protein expression [33], while single-base pair missense mutations in the tyrosine kinase domain lead to ligand-independent signaling [34]. There are three key mutations that are responsible for 85% of *ALK* mutations in NB, which lead to changes in the amino acids R1275, F1174, and F1245 [35]. Activating *ALK* mutations have also been found in other cancer types such as anaplastic thyroid cancer, rhabdomyosarcoma, osteosarcoma, and non-small-cell lung cancer (NSCLC) [30, 36]. In NB, *ALK* mutation, as well as amplification, is correlated with reduced event-free survival and overall survival [35]. *ALK* aberrations were mainly detected in NBs at an advanced stage with an unfavorable outcome [37]. Therefore, they might be related to aggressive forms of NB [38] as *ALK* mutations often occur in *MYCN*-amplified tumors [35]. Mutations in the *ALK* gene were identified to be the major cause of hereditary NB [25] and somatic *ALK* mutations are acquired in 8-10% of sporadic NBs [22, 24, 39]. In relapsed NB there is a high incidence of new *ALK* mutations [40]. *ALK* may serve as a prognostic marker of disease status [35] and represents an attractive target for therapy of NB in a selected group of patients. [25, 35, 39, 41, 42].

Crizotinib, a small molecule-inhibitor of *ALK* showed some promising responses, especially in *ALK* mutated (mut) NSCLC. It remains a promising strategy for *ALK* mut NBs but further investigation of parallel approaches are desirable. [35, 36, 39].

### **1.3 Proteasome inhibitors as therapy option**

In a previous project in the research team of Prof. Remke, performed by Viktoria Marquardt, a clinical inhibitor library was screened on various cell lines including 10 NB cell lines. The results of this screening indicated that *ALK* mut NB cell lines are more sensitive towards proteasome inhibitors compared to *ALK* wildtype (wt) NB cell lines (Figure 1).

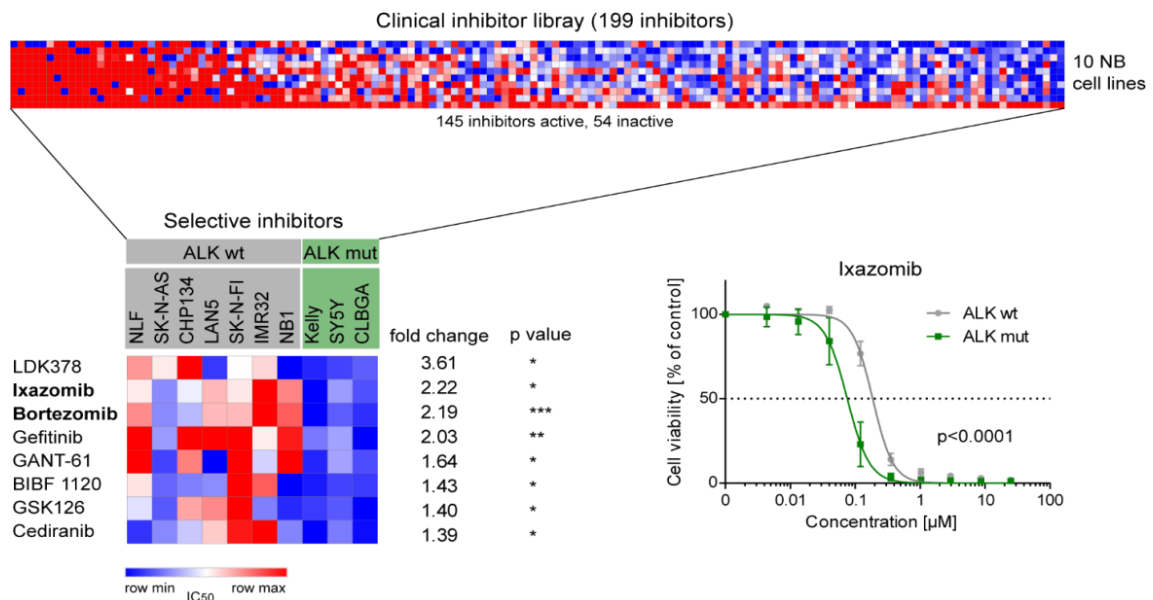


**Figure 1: *ALK* mutated (mut) neuroblastoma (NB) cell lines are more sensitive towards the proteasome inhibitor ixazomib compared to *ALK* wildtype (wt) NB cell lines.** Data provided by Viktoria Marquardt. 199 inhibitors were screened on 10 NB cell lines. Cell viability of *ALK* mut NB cell lines was significantly lower than the cell viability of *ALK* wt NB cell lines.

Proteasome inhibitors approved by the US Food and Drug Administration for clinical application are bortezomib (Velcade, approved in 2003), carfilzomib (Kyprolis, approved in 2012) and ixazomib (Ninlaro, approved in 2015) [43-45]. Bortezomib has been approved for the treatment of multiple myeloma and mantle cell lymphoma [46]. Carfilzomib and ixazomib are used in therapy of multiple myeloma in combination with dexamethasone and lenalidomide [47, 48]. Bortezomib and ixazomib are currently being evaluated in various clinical trials as therapeutic option for other tumor entities [49]. Both, bortezomib and carfilzomib require intravenous or subcutaneous administration, whereas ixazomib is orally available [45-48]. As an oral drug, ixazomib is given as a citrate ester prodrug (MLN9708) that is rapidly hydrolyzed to the active form (MLN2238) [45]. Ixazomib and bortezomib are reversible proteasome inhibitors, carfilzomib in contrast is an irreversible inhibitor of the proteasome [44]. Proteasome inhibitors lead to cell death and affect several pathways utilized by cancer cells. Primarily, they inhibit the proteasome and its downstream events [44]. Their main mechanisms of cytotoxicity are based on suppression of cell survival pathways, activation of apoptotic pathways and enhancement of endoplasmic reticulum stress [43, 50]. Due to a limited spectrum of side effects, proteasome inhibitors are well tolerated [43]. Adverse events after ixazomib treatment include gastrointestinal symptoms or skin rash. The frequency of neuropathy after

ixazomib treatment is much lower than after treatment with bortezomib where neuropathy is one of the main complications [51].

The mechanism of action of proteasome inhibitors is not yet fully understood. Due to the involvement of the proteasome in different regulating mechanisms of the cells, there are different modes of action for proteasome inhibitors, which eventually contribute to cell death. The main events triggered by proteasome inhibitors include the induction of endoplasmic reticulum-stress, the induction of pro-apoptotic proteins, such as p53 and proteins from the Bcl-2 family, induction of autophagy, and the inhibition of the nuclear factor kappa B (NF- $\kappa$ B) pathway. [52]. In 2016, Li et al. reported that ixazomib suppresses cell proliferation and induces cell apoptosis in NB cells [53].

In the previous project, bortezomib and ixazomib were the only proteasome inhibitors included in the clinical inhibitor library (Figure 1). Since oral drug availability is highly desirable in the treatment of children and ixazomib shows better clinical outcomes and reduced toxicities in the treatment of multiple myeloma compared to the first-generation proteasome inhibitor bortezomib [53], we decided to focus our investigations on the orally available ixazomib rather than bortezomib.

#### **1.4 Aim of the thesis**

Currently, the overall survival of patients with NB is generally good, but the five-year overall survival rate of patients with high-risk NB remains below 50%. There are many different studies investigating new therapeutic approaches for patients with high-risk NB. In a previous project, proteasome inhibitors showed a higher sensitivity in *ALK* mut NB cells compared to *ALK* wt NB cells. Therefore, the aim of this thesis was to investigate ixazomib as a therapeutic approach and to analyze the effects of ixazomib treatment in *ALK* mut NB cell lines compared to *ALK* wt NB cell lines. The primary hypothesis was that the novel proteasome inhibitor ixazomib exhibits significant treatment effects in *ALK* mut NB cell lines.

In detail, the following questions should be answered:

1. Does ixazomib treatment influence proliferation and cell viability of *ALK* mut NB cell lines in comparison to *ALK* wt NB cell lines?

2. Does ixazomib treatment induce apoptosis in *ALK* mut NB cell lines in comparison to *ALK* wt NB cell lines?
3. Does ixazomib treatment lead to higher DNA damage in *ALK* mut NB cell lines in comparison to *ALK* wt NB cell lines?
4. What could be the mechanism of action of ixazomib?

## 2 Materials and Methods

### 2.1 Materials

#### 2.1.1 Cell lines

In this thesis, six commercially available human NB cell lines were included. Kelly, SH-SY5Y, CLBGA, IMR 32, SK-N-FI cell lines were kindly provided by Prof. Alex Schramm from Essen. NBL-S cell line was kindly provided by Prof. Till Milde from Heidelberg. All the cell lines are listed in Table 1.

**Table 1: Cell lines**

ID	<i>ALK</i> mutation	<i>ALK</i> amplification	<i>MYCN</i> status	<i>TERT</i> mutation	<i>TP53</i> mutation
IMR 32	Wildtype	Partial [37]	Amplified	No	No
NBL-S	Wildtype	No	Not amplified	N/A	No
SK-N-FI	Wildtype	No	Not amplified	No	Loss of function M246R
Kelly	F1174L	No	Amplified	No	P177T
CLBGA	R1275Q	No	Not amplified	Rearrangement [54]	N/A
SH-SY5Y	F1174L	No	Not amplified	C228T mutation [55]	No

(*TERT*: Telomerase reverse transcriptase; N/A: not available)

#### 2.1.2 Media and supplements

The various cell culture media and supplements used in this thesis are summarized in Table 2.

**Table 2: Media and supplements**

Name	Company	Reference #
Dimethylsulfoxide (DMSO)	AppliChem, Darmstadt, Germany	A3672
Fetal bovine serum (FBS), heat inactivated	Sigma-Aldrich, Taufkirchen, Germany	F9665
Iscove's modified dulbecco's medium (IMDM 1x)	Gibco, Darmstadt, Germany	12440053
Phosphate buffered saline (PBS)	Sigma-Aldrich, Taufkirchen, Germany	D8537
RPMI 1640 (1X)	Gibco, Darmstadt, Germany	31870025

### 2.1.3 Buffers

The various buffers used in this thesis are summarized in Table 3.

**Table 3: Buffers**

Name	Compositition
Blocking Solution	5% Bovine Serum Albumin (BSA) dissolved in TBS-T
M-MLV RT 5x Buffer	Promega, Madison, USA #M531A
Novex Tris-Glycine SDS running buffer 10x	Thermo Scientific, Bremen, Germany #LC2675
PBS-T	PBS; 0.1% Tween 20
RIPA Lysis Buffer (10x)	Sigma-Aldrich, Taufkirchen, Germany (Reference #20-188)
Samplebuffer (5x)	1 M Tris/HCL (pH 6.8); 62.5% (v/v) Glycerin; 10% (w/v) sodium dodecyl sulfate (SDS)
TBS-T	20 mM Tris (pH 7.5); 150 mM NaCl; 0.1% Tween 20
Transfer Buffer (10x)	25 mM Tris; 190 mM Glycine

(M-MLV RT: Moloney Murine Leukemia Virus Reverse Transcriptase; PBS-T: phosphate-buffered saline with Tween; RIPA: Radioimmunoprecipitation assay; TBS-T: Tris-buffered saline with Tween)

### 2.1.4 Chemicals

The chemicals used in this thesis are summarized in Table 4.

**Table 4: Chemicals**

<b>Name</b>	<b>Company</b>	<b>Reference #</b>
16% Formaldehyde Solution (w/v)	Thermo Fisher Scientific, Bremen, Germany	28908
2-Propanol	VWR Chemicals, Fontenay-sous-Bois, France	20.842.330
BSA (Albumin Fraktion V)	Roth, Karlsruhe, Germany	8076.4
Crystal Violet	Fluka, Schwerte, Germany	32675
Ethanol (EtOH) Absolute	VWR Chemicals, Fontenay-sous-Bois, France	20.821.330
Formalin 10% Neutral Buffered	ScyTek Laboratories, Hamburg, Germany	FRN999
Glycine	Roth, Karlsruhe, Germany	3908.2
Powdered milk	Roth, Karlsruhe, Germany	T145.2
Tris	Roth, Karlsruhe, Germany	5429.1
Triton X 100	Roth, Karlsruhe, Germany	6683.1
Tween® 20	Merck, Darmstadt, Germany	8.221.840.500

### 2.1.5 Specific reagents and other materials

The specific reagents and other materials used in this thesis are summarized in Table 5.

**Table 5: Specific reagents and other materials**

<b>Name</b>	<b>Company</b>	<b>Reference #</b>
Amersham™ Protran™ 0.45µm Nitrocellulose Blotting Membrane	GE Healthcare, Chicago, USA	10600002
dNTP Mix	Promega, Madison, USA	U151B
DTT 0.1M	Thermo Scientific, Bremen, Germany	P/N y00147
Goat Serum	Sigma-Aldrich, Taufkirchen, Germany	G9023
Laminin	Corning, Wiesbaden, Germany	354232
Novex™ WedgeWell™ 4-12% Tris-Glycine Gel	Invitrogen, Darmstadt, Germany	XP04122BOX

Oligo(dT) Primer				Promega, Madison, USA		C110A
PageRuler™ Ladder	Prestained Protein			Thermo Fisher Scientific, Germany	Bremen,	26616
Phosphatase Inhibitor Cocktail				Roche, Basel, Switzerland		4906837001
Precision Blue™ Dye	Real-Time PCR			Bio-Rad, Hercules, USA		172-5555
Propidium Iodide (PI)				Sigma-Aldrich, Taufkirchen, Germany		P4864
Protease Inhibitor Cocktail				Roche, Basel, Switzerland		4693132001
Protein Assay Concentrate	Dye Reagent			Bio-Rad, Hercules, USA		500-0006
Protein standard				Sigma-Aldrich, Taufkirchen, Germany		P0914-10AMP
Random Primer				Promega, Madison, USA		C118A
SuperSignal™ Maximum Sensitivity Substrate	West Femto			Thermo Fisher Scientific, Germany	Bremen,	C118A
TaqMan™ with UNG	Universal Master Mix II,			Thermo Scientific, Bremen, Germany		4440038
Trypan Blue Solution				Sigma-Aldrich, Taufkirchen, Germany		T8154
Trypsin-EDTA (1x)				Gibco, Darmstadt, Germany		25300054
Vectashield Mounting Medium for Fluorescence				Vector Laboratories, Eching, Germany		H-1000
Whatman™ Gel Blot Paper				GE Healthcare, Chicago, USA		GB003

(dNTP: Deoxyribonucleotide triphosphate; DTT: Dithiothreitol; PCR: Polymerase chain reaction; EDTA: Ethylenediaminetetraacetic acid)

### 2.1.6 Primers

The primers summarized in Table 6 were used for TaqMan® real-time PCR and were obtained from IDT Integrated DNA Technologies, Iowa, USA. Primers were provided as PrimeTime Std qPCR Assays and were resuspended in IDTE buffer to a 20x working solution.

**Table 6: Primer for TaqMan® real-time PCR**

Name	Assay name
ACTB	Hs.PT.39a.22214847

<i>FOS</i>	Hs.PT.58.15540029
<i>GAPDH</i>	Hs.PT.39a.22214836
<i>GUSB</i>	Hs.PT.58v.27737538
<i>IKBKB</i>	Hs.PT.58.40427794
<i>NF-κB1</i>	Hs.PT.58.20344216
<i>NF-κB2</i>	Hs.PT.58.46592905
<i>PPIA</i>	Hs.PT.39a.22214851
<i>RELA</i>	Hs.PT.58.22880470
<i>RELB</i>	Hs.PT.58.2898589
<i>RPL13</i>	Hs.PT.58.26748094
<i>TGM2</i>	Hs.PT.58.1937434

(*ACTB*: actin beta, *FOS*: fos proto-oncogene, *AP-1* transcription factor subunit, *GAPDH*: glyceraldehyde-3-phosphate dehydrogenase, *GUSB*: glucuronidase beta, *IKBKB*: inhibitor of nuclear factor kappa B kinase subunit beta, *NF-κB1*: nuclear factor kappa B subunit 1, *NF-κB2*: nuclear factor kappa B subunit 2, *PPIA*: peptidylprolyl isomerase A, *RELA*: RELA proto-oncogene, *NF-κB* subunit, *RELB*: RELB proto-oncogene, *NF-κB* subunit, *RPL13*: ribosomal protein L13, *TGM2*: transglutaminase 2)

## 2.1.7 Enzymes

The enzymes used in this thesis are listed in Table 7.

**Table 7: Enzymes**

<b>Name</b>	<b>Company</b>	<b>Reference #</b>
M-MLV Reverse Transcriptase	Promega, Madison, USA	M368C
RNase A (DNase-free)	AppliChem, Darmstadt, Germany	A3832
RNasin® Ribonuclease Inhibitor	Promega, Madison, USA	N261B

## 2.1.8 Antibodies

### 2.1.8.1 Western blot analysis

All antibodies for Western blot analysis used in this thesis are listed in Table 8.

**Table 8: Antibodies for Western blot analysis**

Name	Company	Dilution	Reference #
Anti-mouse IgG, HRP-linked Antibody	Cell Signaling Technology, Cambridge, UK	1:1000	7076
Anti-rabbit IgG, HRP-linked Antibody	Cell Signaling Technology, Cambridge, UK	1:1000	7074
beta-Tubulin (D2N5G) Rabbit (HRP conjugate)	Cell Signaling Technology, Cambridge, UK	1:1000	56739
GAPDH (14C10) Rabbit mAb	Cell Signaling Technology, Cambridge, UK	1:1000	2118S
IKK $\alpha$ (3G12) Mouse mAb	Cell Signaling Technology, Cambridge, UK	1:1000	11930
IKK $\beta$ (D30C6) Rabbit mAb	Cell Signaling Technology, Cambridge, UK	1:1000	8943
I $\kappa$ B $\alpha$ (L35A5) Mouse mAb (Amino-terminal Antigen)	Cell Signaling Technology, Cambridge, UK	1:1000	4814
NF- $\kappa$ B Sampler Kit	Cell Signaling Technology, Cambridge, UK	1:1000	9936
NF- $\kappa$ B p65 (D14E12) XP <sup>®</sup> Rabbit mAb	Cell Signaling Technology, Cambridge, UK	1:1000	8242
Phospho- I $\kappa$ B $\alpha$ (Ser32) (14D4) Rabbit mAb	Cell Signaling Technology, Cambridge, UK	1:1000	2859
Phospho- NF- $\kappa$ B p65 (Ser536) (93H1) Rabbit mAb	Cell Signaling Technology, Cambridge, UK	1:1000	3033
Phospho-IKK $\alpha/\beta$ (Ser176/180) (16A&) Rabbit mAb	Cell Signaling Technology, Cambridge, UK	1:1000	2697

(HRP: Horseradish peroxidase; IKK: I $\kappa$ B kinase; I $\kappa$ B $\alpha$ : nuclear factor of kappa light polypeptide gene enhancer, alpha; mAb: monoclonal antibodies)

### 2.1.8.2 Immunofluorescence analysis

All antibodies for immunofluorescence analysis used in this thesis are listed in Table 9.

**Table 9: Antibodies for immunofluorescence analysis**

Name	Company	Dilution	Reference #
4',6-diamidino-2-phenylindole (DAPI)	Thermo Fisher Scientific, Bremen, Germany	1:1000	62248
Anti-mouse IgG Fab2 Alexa Fluor® 488	Cell Signaling Technology, Cambridge, UK	1:500	4408S
Anti-rabbit IgG Fab2 Alexa Fluor® 594	Cell Signaling Technology, Cambridge, UK	1:500	8889S
Ki-67 (D385) Rabbit mAb	Cell Signaling Technology, Cambridge, UK	1:400	9129S
P-Histone H2A.X (S139) (D7T2V) Mouse mAb	Cell Signaling Technology, Cambridge, UK	1:100	80312S

### 2.1.9 Commercially available kits

The commercially available kits used in this thesis are summarized in Table 10.

**Table 10: Commercially available kits**

Name	Company	Reference #
Caspase-Glo® 3/7 Assay	Promega, Madison, USA	G8091
CellTiter-Glo® Luminescent Cell Viability Assay	Promega, Madison, USA	G7573
Clickt-iT™ EdU Alexa Fluor™ 488 Imaging Kit	Thermo Fisher Scientific, Bremen, Germany	C10337
Fluorescein isothiocyanat (FITC) Annexin V	BD Biosciences, San Jose, USA	556419 (FITC Annexin V) 556454 (Annexin V Binding Buffer)
Maxwell® RSC simplyRNA Cells Kit	Promega, Madison, USA	AS1340

(EdU: 5-ethynyl-2'deoxyuridine; RSC: Rapid Sample Concentrator)

### 2.1.10 Other consumables

All other consumables used in this thesis are summarized in Table 11.

**Table 11: Other consumables**

Name	Company	Reference #
5 ml Polypropylene Round-Bottom Tube	Corning, Wiesbaden, Germany	352053

Cell culture flasks (25 cm <sup>2</sup> & 75 cm <sup>2</sup> )	Greiner Bio-One, Solingen, Germany	690175 658175
Cell culture flasks (25 cm <sup>2</sup> & 75 cm <sup>2</sup> )	Corning, Wiesbaden, Germany	3289 3290
Cell culture plates (96-well, 48-well & 6-well)	Greiner Bio-One, Solingen, Germany	655185 677180 657185
Cell Strainer 70 µm Nylon	Corning, Wiesbaden, Germany	431751
Centrifuge tubes (1.5 ml & 2 ml)	Eppendorf, Hamburg, Germany	30.123.328 30.123.344
Cover Slips (24 x 50 mm)	VWR, Darmstadt, Germany	
Falcon tubes (15 ml & 50 ml)	Greiner Bio-One, Solingen, Germany	188271 227261
Flitorpur V50 500ml, 0,22 µm	Sarstedt, Nümbrecht, Germany	833941001
Hard-Shell® 384-Well PCR Plates	Bio-Rad, Hercules, USA	HSP3805
Microseal® `B` seal Seals	Bio-Rad, Hercules USA	MSB1001
Nunc™ CryoTube™ Vials	Thermo Fisher Scientific, Bremen, Germany	374115
Nunc™ Lab-Tek™ II Chamber Slide™ System 8-well Glass Slide	Thermo Fisher Scientific, Bremen, Germany	154534
PCR tube strips 0.2 ml	Eppendorf, Hamburg, Germany	0030 124.359
White 96 well plate, nontreated	Thermo Fisher Scientific, Bremen, Germany	236105
White 96-well plate, Nunclon™ Delta Surface	Thermo Fisher Scientific, Bremen, Germany	136101

### 2.1.11 Devices

The devices and laboratory equipment used in this thesis are summarized in Table 12.

**Table 12: Devices**

Name	Company
ApoTome.2	Zeiss, Oberkochen, Germany
Axio Observer.Z1	Zeiss, Oberkochen, Germany

Axio Vert.A1	Zeiss, Oberkochen, Germany
CFX384™ Real-Time System	Bio-Rad, Hercules, USA
CO2 incubator for cell culture (HERA cell)	Heraeus, Hanau, Germany
Cryo-Safe™ Cooler	Bel-Art Products, Warminster, USA
CytoFLEX	Beckman Coulter, Krefeld, Germany
GeneAmp® PCR System 2700	Applied Biosystems, Foster City, USA
LAS-3000 mini 2UV Transilluminator	Fujifilm, Düsseldorf, Germany
Maxwell Rapid Sample Concentrator (RSC)	Promega, Madison, USA
Megafuge 3.0R	Heraeus, Hanau, Germany
Milli-Q Integral 15	Merck, Darmstadt, Germany
Mini Blot Module	Invitrogen, Darmstadt, Germany
Mini Gel Tank	Invitrogen, Darmstadt, Germany
Mini-Rocker Shaker	Peqlab, Darmstadt, Germany
Multifuge X3R	Thermo Scientific, Bremen, Germany
NanoDrop Spectrophotometer ND-1000	Peqlab, Darmstadt, Germany
Neubauer counting chamber	Brand, Wertheim, Germany #718605
peqTWIST	Peqlab, Darmstadt, Germany
PerfectSpin 24R Refrigerated Microcentrifuge	Peqlab, Darmstadt, Germany
Roller Mixer (SRT6)	Stuart, Stone, UK
Spark 10M Microplate Reader	Tecan, Männedorf, Schweiz
ThermoMixer C	Eppendorf, Hamburg, Germany

### 2.1.12 Software

All different kinds of software used for data analysis in this thesis are listed in Table 13.

**Table 13: Software**

<b>Name</b>	<b>Company</b>
Bio-Rad CFX Manager	Bio-Rad, Hercules, USA
CytExpert	Beckman Coulter, Krefeld, Germany
GraphPad Prism 5.03	GraphPad Software, San Diego, USA
Ingenuity Pathway Analysis	Qiagen, Hilden, Germany
Spark Control	Tecan, Männedorf, Schweiz

## **2.2 Methods**

### **2.2.1 Cell cultivation**

All cell lines were incubated at 37 °C in a 5% CO<sub>2</sub> atmosphere and maintained as monolayer cultures. CLBGA, Kelly, SH-SY5Y, IMR 32, SK-N-FI were kept in complete medium, consisting of RPMI 1640 supplemented with 20% FBS. NBL-S were kept in complete medium, consisting of IMDM supplemented with 20% FBS. All cell lines were passaged with Trypsin-EDTA and split once or twice a week in ratios from 1:2 – 1:10.

### **2.2.2 Cell cryopreservation**

Cells were harvested and centrifuged at 300-times gravity (xg) at room temperature (RT) for 5 min. Cells were resuspended in 800 µl cryomedium, consisting of complete medium supplemented with 10% DMSO and transferred into CryoTube™ vials. Cells were frozen at 1 °C/min in a CryoSafe™ cooler filled with 2-propanol at -80 °C for at least 24 h. For long term storage, cells were kept in the gas phase of liquid nitrogen. For cell cultivation, cryovials were thawed at 37 °C and centrifuged at 300 xg at RT for 5 min to replace the freezing medium with fresh complete medium.

### **2.2.3 Dilution series**

In order to ensure exponential growth for 96 h, the optimal cell number for each cell line and plate format was determined by performing dilution series. For this, cells were harvested and stained with Trypan Blue Solution in a 1:1 dilution. Following, cells were counted using a Neubauer counting chamber and then seeded into 6-well, 48-well and 96-well plates with different cell numbers per well. The optimal cell numbers obtained for each cell line on each plate format are listed in Table 14.

**Table 14: Dilution series**

	<b>6-well Plate</b>	<b>48-/8-well Plate</b>	<b>96-well Plate</b>
	<b>Cells/Well</b>	<b>Cells/Well</b>	<b>Cells/Well</b>
Kelly	25 x 10 <sup>4</sup>	3 x 10 <sup>4</sup>	1.5 x 10 <sup>4</sup>
SH-SY5Y	75 x 10 <sup>4</sup>	8.5 x 10 <sup>4</sup>	1.8 x 10 <sup>4</sup>
CLBGA	79.5 x 10 <sup>4</sup>	15 x 10 <sup>4</sup>	3.5 x 10 <sup>4</sup>
IMR 32	50 x 10 <sup>4</sup>	5 x 10 <sup>4</sup>	1.8 x 10 <sup>4</sup>
SK-N-FI	50 x 10 <sup>4</sup>	5 x 10 <sup>4</sup>	1.2 x 10 <sup>4</sup>
NBL-S	50 x 10 <sup>4</sup>	5.5 x 10 <sup>4</sup>	1.5 x 10 <sup>4</sup>

#### **2.2.4 Treatment with ixazomib**

For all the following experiments, the cells were seeded onto the specific plate according to their cell number. After 24 h, cells were treated with ixazomib or DMSO as negative control. The Kelly cell line was always treated with 25 nM ixazomib whereas all other cell lines were treated with 50 nM ixazomib. For some of the experiments, the cells were also treated with 500 nM or 1  $\mu$ M staurosporine as a positive control. Ixazomib, DMSO and staurosporine were diluted in PBS.

#### **2.2.5 Cell proliferation**

For the analysis of cell proliferation, EdU cell proliferation assay was performed. Cells were seeded on Nunc™ Lab-Tek™ II Chamber Slide™ System 8-well glass slides. The next day, cells were treated with ixazomib or DMSO as a negative control as described above (2.2.4). After 24 h, 48 h and 72 h of treatment, 10  $\mu$ M EdU was added to each well. After incubation (5 h at 37 °C), cells were fixed using 4% formaldehyde in PBS (15 min at RT) and permeabilized using 0.5% Triton® X-100 in PBS (20 min at RT). In between, cells were washed twice with 3% BSA in PBS. Subsequently, EdU detection was performed using the Click-iT® EdU Alexa Fluor™ 488 Imaging Kit according to the manufacturer's protocol. DNA was counterstained using DAPI before slides were covered with cover slips using Vectashield Mounting Medium for Fluorescence. Images were taken using Axio Observer.Z1 fluorescence microscope with a 40x oil objective from Zeiss. For the quantification of proliferating cells, at least five randomly selected microscopic fields per 8-well were examined. The percentage of proliferating cells was calculated by counting the number of DAPI-labeled cells and the number of EdU-labeled cells and taking its ratio afterwards.

### **2.2.6 Crystal violet staining**

To visualize the effect of ixazomib on the cells, crystal violet staining was performed. After 24 h, cells were seeded into 6-well plates and treated with ixazomib or DMSO as a negative control as described above (2.2.4). After 72 h, cells were washed with PBS, fixed with 10% formalin (30 min at RT) and stained with 0.1% crystal violet (1 h at RT). Afterwards, cells were washed with double distilled water (ddH<sub>2</sub>O) and images were acquired.

### **2.2.7 Cell viability**

For the determination of cell viability, cells were seeded into 96-well plates. After 24 h of incubation, cells were treated with ixazomib or DMSO as a negative control as described above (2.2.4). After 72 h, the CellTiter-Glo<sup>®</sup> Luminescent Cell Viability Assay was performed according to the manufacturer's protocol. The CellTiter-Glo<sup>®</sup> Reagent was diluted (1:2 v/v) with PBS. Luminescence was measured using Spark 10M Microplate Reader.

### **2.2.8 Annexin V**

For the analysis of apoptosis, Annexin V staining was performed. Cells were seeded into 6-well plates. After 24 h or 72 h, cells were treated with ixazomib, DMSO as a negative control or with 1  $\mu$ M staurosporine as a positive control as described above (2.2.4). After 72 h of treatment with ixazomib, DMSO or staurosporine, cells were stained with FITC Annexin V and PI according to the manufacturer's protocol and analyzed via FACS using the CytoFLEX from Beckman Coulter.

### **2.2.9 Caspase 3/7**

To detect caspase 3/7 activity in ixazomib treated cells, cells were seeded into 96-well plates. After 24 h of incubation, cells were treated with ixazomib, DMSO as a negative control or 500 nM staurosporine as a positive control as described above (2.2.4). After 24 h, the Caspase-Glo<sup>®</sup> 3/7 Assay was performed according to the manufacturer's protocol. Luminescence was measured using Spark 10M Microplate Reader.

### **2.2.10 DNA damage**

For the analysis of DNA damage, an immunofluorescence staining was performed with the  $\gamma$ H2A.X antibody. 24 h after cells were seeded on Nunc™ Lab-Tek™ II Chamber Slide™ System 8-well glass slides, cells were treated with ixazomib or DMSO as a negative control, as described above (2.2.4). After 48 h, cells were fixed with 4% PFA diluted in PBS (20 min at RT) and permeabilized with 0.5% Triton® X100 (20 min at RT). Next, unspecific binding sites were blocked (1 h at RT) with blocking solution consisting of 1% BSA and 3% goat serum diluted in PBS. Afterwards, cells were stained with primary antibodies  $\gamma$ H2A.X (diluted 1:100 in blocking solution) and Ki-67 (diluted 1:400 in blocking solution) and incubated overnight at 4 °C. After washing three times with PBS, cells were stained with secondary antibodies (anti-rb Alexa 594 and anti-ms Alexa 488, both diluted 1:500 in blocking solution) for 45 min at RT in the dark. Before and after DNA staining with DAPI, cells were washed three times with PBS. Finally, the slides were covered with cover slips using Vectashield Mounting Medium for Fluorescence. Images were taken using Axio Observer.Z1 fluorescence microscope with a 40x oil objective and the ApoTome.2 from Zeiss. For the quantification of cells undergoing DNA damage, at least five randomly selected microscopic fields per well were examined. The percentage of DNA damaged cells was calculated by counting the number of DAPI-labeled cells and the number of  $\gamma$ H2A.X-labeled cells and taking its ratio afterwards.

### **2.2.11 Ingenuity pathway analysis**

Ingenuity pathway analysis (IPA, Qiagen) was performed with the kind help of Daniel Picard. IPA was conducted using genes with significant differential expression ( $p \leq 0.05$  and fold change  $\pm 2$ ). Ingenuity pathway analysis default settings were used except for Knowledge Base where high confidence experimental knowledge was included. Genes were considered significant if they had a p value  $< 0.05$  and a fold change  $\pm 2$ , for a total of 60 differentially expressed genes. Additionally, for upstream regulators, we filtered out biological drugs, all chemical and miRNA entries.

For IPA, processed RNA sequencing data for GSE89413 was downloaded from R2 data portal (<https://hgserver1.amc.nl/cgi-bin/r2/main.cgi>).

For the ixazomib pathways analysis, we used the ixazomib knowledge from IPA (white) and then used the "grow" function to add relationships based on differentially regulated genes found in our datasets (red up, blue down).

### 2.2.12 RNA extraction, cDNA synthesis and quantitative real-time PCR

Extraction of RNA was conducted using the Maxwell RSC Instrument as per manufacturer's instruction. RNA was measured using the NanoDrop Spectrophotometer ND-1000. cDNA was synthesized from 0.5 µg total RNA using M-MLV Reverse Transcriptase according to manufacturer's instructions. Table 15, 16 and 17 show the compositions and conditions for cDNA synthesis. GeneAmp® PCR System 2700 was used for the different incubation conditions.

**Table 15: Composition of Mix I**

	Mix I
RNA	0.5 µg
Random/Oligo(dT) Primer Mix	0.5 µl
H <sub>2</sub> O	Add 14 µl

Mix I was incubated for 5 min at 70 °C, following by at least 1 min at 4 °C.

**Table 16: Composition of Mix II**

	Mix II
M-MLV RT 5x Buffer	5 µl
dNTP	1.25 µl
M-MLV Reverse Transcriptase	1 µl
RNasin® Ribonuclease Inhibitor	1 µl
H <sub>2</sub> O	2.75 µl

11 µl of Mix II were added to Mix I and incubated under following conditions:

**Table 17: Conditions for cDNA synthesis**

Condition	
1	25 °C for 10 min
2	50 °C for 50 min
3	70 °C for 15 min
4	4 °C ∞

Gene expression was verified by quantitative real-time PCR using the CFX384TM Real-Time System from Bio-Rad. For normalization *PPIA*, *GUSB*, *GAPDH* and *ACTB* served as housekeeping genes. Samples were quantified in triplets. The  $\Delta\Delta CT$  method was used for the relative quantification of PCR products. Table 18 and 19 show the compositions and conditions for real-time PCR.

**Table 18: Real-time PCR compositions**

	TaqMan®
Master Mix	5 $\mu$ l
Primer Mix	0.5 $\mu$ l
H <sub>2</sub> O	3.5 $\mu$ l
cDNA	1 $\mu$ l

**Table 19: Real-time PCR conditions**

TaqMan®	
1	50 °C for 2 min
2	95 °C for 10 min
3	95 °C for 00:15 min
4	60 °C for 1 min
5	GOTO 3, x39 cycles

### 2.2.13 Cell lysis, protein extraction and Western blot

Protein was extracted using RIPA Lysis Buffer supplemented with protease and phosphatase inhibitor cocktail. Protein was quantified with the Bradford method using the Protein Assay Dye Reagent Concentrate [56]. Samples were separated by SDS polyacrylamide gel electrophoresis (SDS-PAGE, 15 min at 65 V, followed

by 90 min at 130 V) using Novex™ WedgeWell™ 4-12% Tris-Glycine Gels and then blotted onto Amersham™ Protran™0.45 µm Nitrocellulose Blotting Membrane (1 h at 10 V) using the Mini Gel Tank and Blot Module from Thermo Fisher Scientific. To block unspecific binding sites, membranes were incubated (1 h) in blocking solution composed of 5% BSA diluted in TBS-T. Subsequently, the membranes were incubated with the primary antibodies, diluted in blocking solution (overnight at 4 °C). Following, the membranes were washed three times with TBS-T (5 min at RT), incubated with the secondary antibodies, diluted in blocking solution (1 h at RT) and washed again three times with TBS-T. To make the proteins visible, SuperSignal™ West Femto Maximum Sensitivity Substrate was used before the detection in the LAS-3000 mini 2UV Transilluminator by Fujifilm.

#### **2.2.14 Statistical analyses**

Statistical analyses were performed using GraphPad Prism 5.03 (GraphPad Software, San Diego, USA). All data are presented as mean ±SEM of at least three independent experiments, unless mentioned otherwise. Comparisons between groups were made employing t-test as appropriate. p-values ≤0.05 were considered significant.

### 3 Results

#### 3.1 Treatment with ixazomib reduces the oncophenotype in *ALK* mutated neuroblastoma cells

Data from Muz et al. showed that ixazomib leads to decreased cell viability and induces apoptosis in NB cell lines [57]. To investigate whether *ALK* mut NB cell lines are even more sensitive towards ixazomib treatment in comparison to *ALK* wt NB cell lines, six different human NB cell lines (three *ALK* mut versus three *ALK* wt cell lines, Table 1) were treated with ixazomib. Next, the effect was functionally analyzed by performing several assays regarding cell proliferation, cell viability, apoptosis and DNA damage.

For the EdU cell proliferation assay, cells were treated with different concentrations of ixazomib (75 nM, 100 nM, 125 nM). The concentrations were chosen according to the IC<sub>50</sub> values that were detected in the previously performed high-throughput drug screening (Figure 1). After ixazomib treatment, decreased cell proliferation was observed in the *ALK* mut NB cell lines Kelly and SH-SY5Y. In contrast, the *ALK* wt NB cell line IMR 32 was still proliferating (Figure 2).

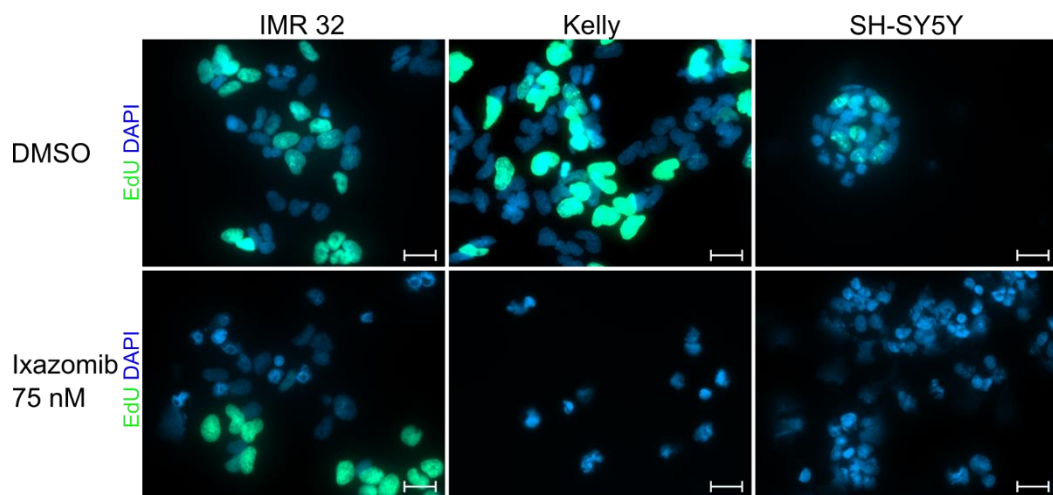


**Figure 2: Ixazomib treatment inhibits cell proliferation in *ALK* mutated (mut) neuroblastoma (NB) cell lines.** Ixazomib and DMSO treated IMR 32 (*ALK* wildtype (wt)), Kelly and SH-SY5Y (*ALK* mut) cells were treated with ixazomib. After 72 h, treated cells were incubated with 10  $\mu$ M EdU for 5 h. Subsequently, cells were fixed and EdU (modified thymidine analogue) was detected using Alexa Fluor™ 488 azide (green). Cells were counterstained with 4',6-diamidino-2-phenylindole (DAPI, blue). Representative immunofluorescence images of treatment with 75 nM ixazomib and DMSO are depicted. The scale bar corresponds to 20  $\mu$ m. Images were taken using an 40x objective. The assay was performed with the depicted three cell lines only.

Since 75 nM of ixazomib already led to a tremendous amount of cell death in *ALK* mut NB (data not shown), suitable ixazomib concentrations needed to be determined for further experiments. For this, crystal violet staining was performed once after treatment of all cell lines with different ixazomib concentrations. As demonstrated in Figure 3, the *ALK* wt NB cells IMR 32, NBL-S and SK-N-FI were clearly viable in contrast to the *ALK* mut NB cells Kelly, CLBGA and SH-SY5Y after ixazomib treatment. Based on these experiments, the ixazomib concentrations of 25 nM and 50 nM were selected for further investigation.

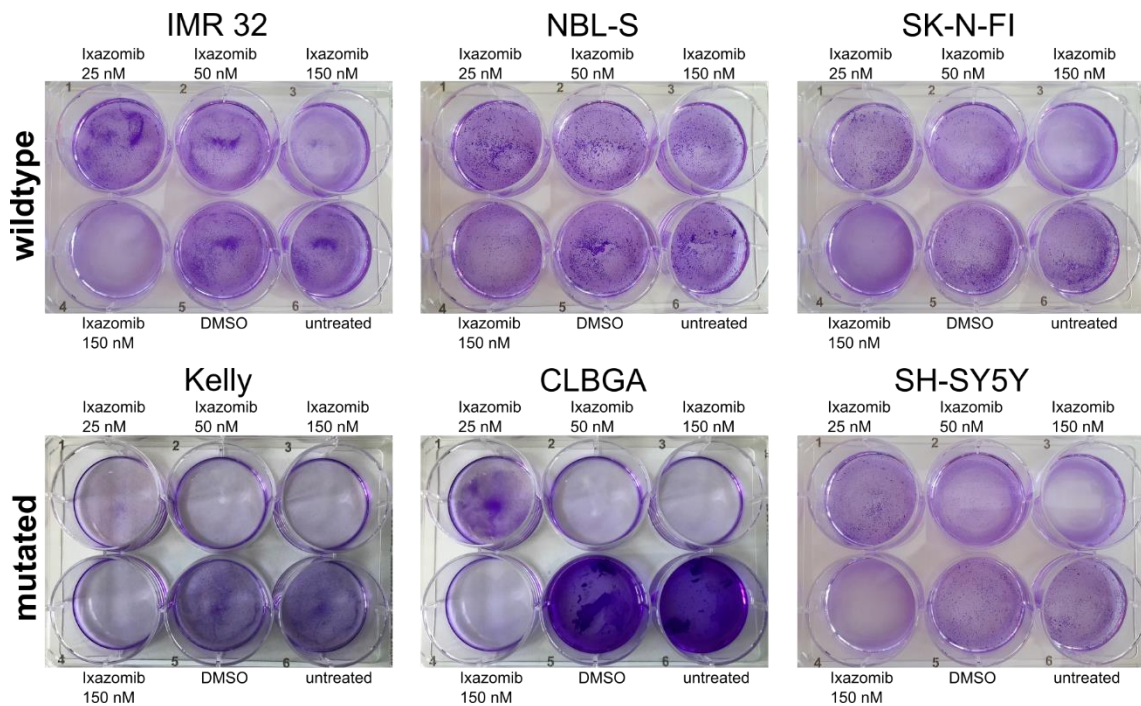


**Figure 3: *ALK* wildtype (wt) neuroblastoma (NB) cell lines are highly sensitive to ixazomib treatment.** All NB cell lines were treated with 25 nM (well 1), 50 nM (well 2), 100 nM (well 3) and 150 nM (well 4) ixazomib and 150 nM DMSO as negative control (well 5). One well per cell line was left untreated (well 6) as a growth control. After 72 h, cells were washed, fixed and stained with 0.1% crystal violet for 1 h. Representative images of each cell line are depicted. Crystal violet staining was performed once.

### 3.1.1 Decreased cell viability in *ALK* mutated neuroblastoma cell lines after ixazomib treatment

To confirm the hypothesis that *ALK* mut NB cell lines are more sensitive to ixazomib treatment in comparison to *ALK* wt cell lines, a cell viability assay based on luminescence was performed. Ixazomib treatment led to significant reduction of cell viability of 44 – 54% in *ALK* mut cell lines (Figure 4, B). Minor treatment effects were also observed in *ALK* wt NB cells (NBL-S (6%), SK-N-FI (33.5%))

(Figure 4, A) indicating that ixazomib may also have a therapeutic function independent from the *ALK* status.

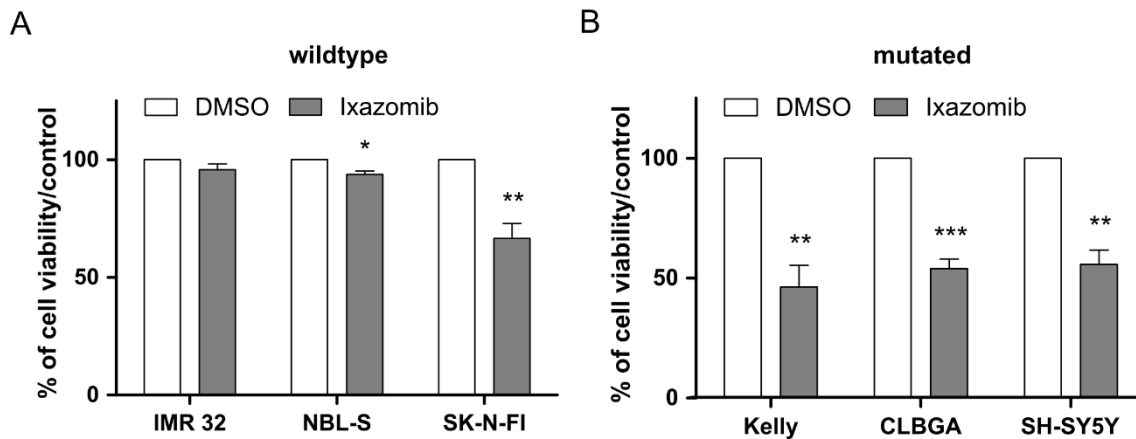


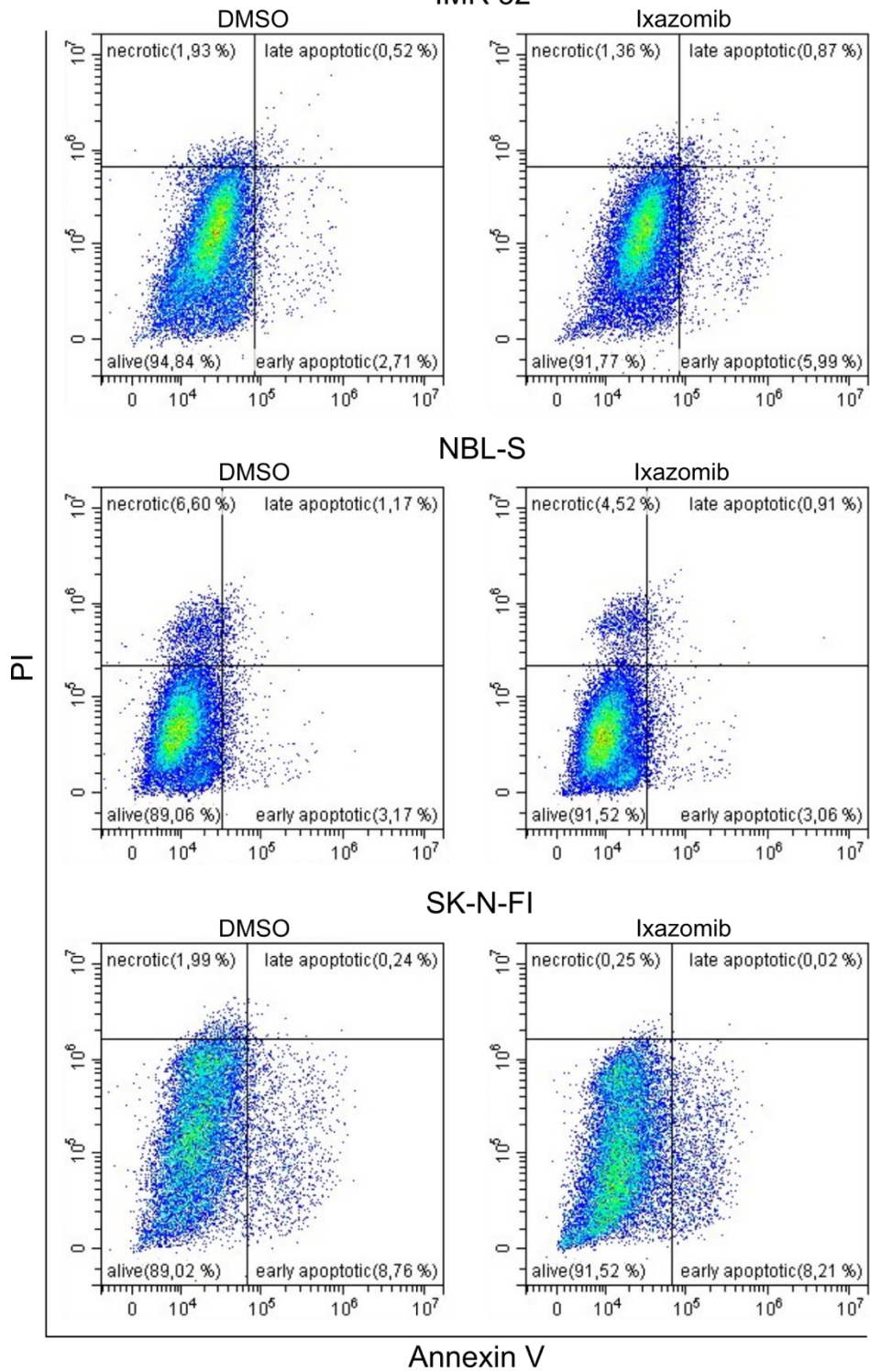
**Figure 4: Reduced cell viability in *ALK* mutated (mut) neuroblastoma (NB) cell lines after ixazomib treatment.** Cells were seeded in complete medium into 96-well plates and treated with ixazomib (25 nM Kelly cells; 50 nM all other cell lines) or DMSO as a negative control. After 72 h, the *CellTiter-Glo*<sup>®</sup> *Luminescent Cell Viability* assay was performed. Luminescence was measured using a Spark 10M Microplate Reader. (A, B) Bar graphs represent the percentage of cell viability of ixazomib treated cells in comparison to the DMSO control. Values shown represent mean  $\pm$ SEM of five independent replicates. \* $p < 0.05$ ; \*\* $p < 0.01$ ; \*\*\* $p < 0.001$  (student's t-test).

### 3.1.2 Increased apoptosis in *ALK* mutated neuroblastoma cell lines after ixazomib treatment compared to *ALK* wildtype cell lines

To further investigate whether the ixazomib-induced loss of cell viability in *ALK* mut NB cell lines was due to increased apoptosis, Annexin V staining and a Caspase 3/7 assay were performed. An increase in apoptotic cells (Annexin V + PI +) was observed following ixazomib treatment in *ALK* mut NB cell lines (Figure 5).

wildtype

IMR 32



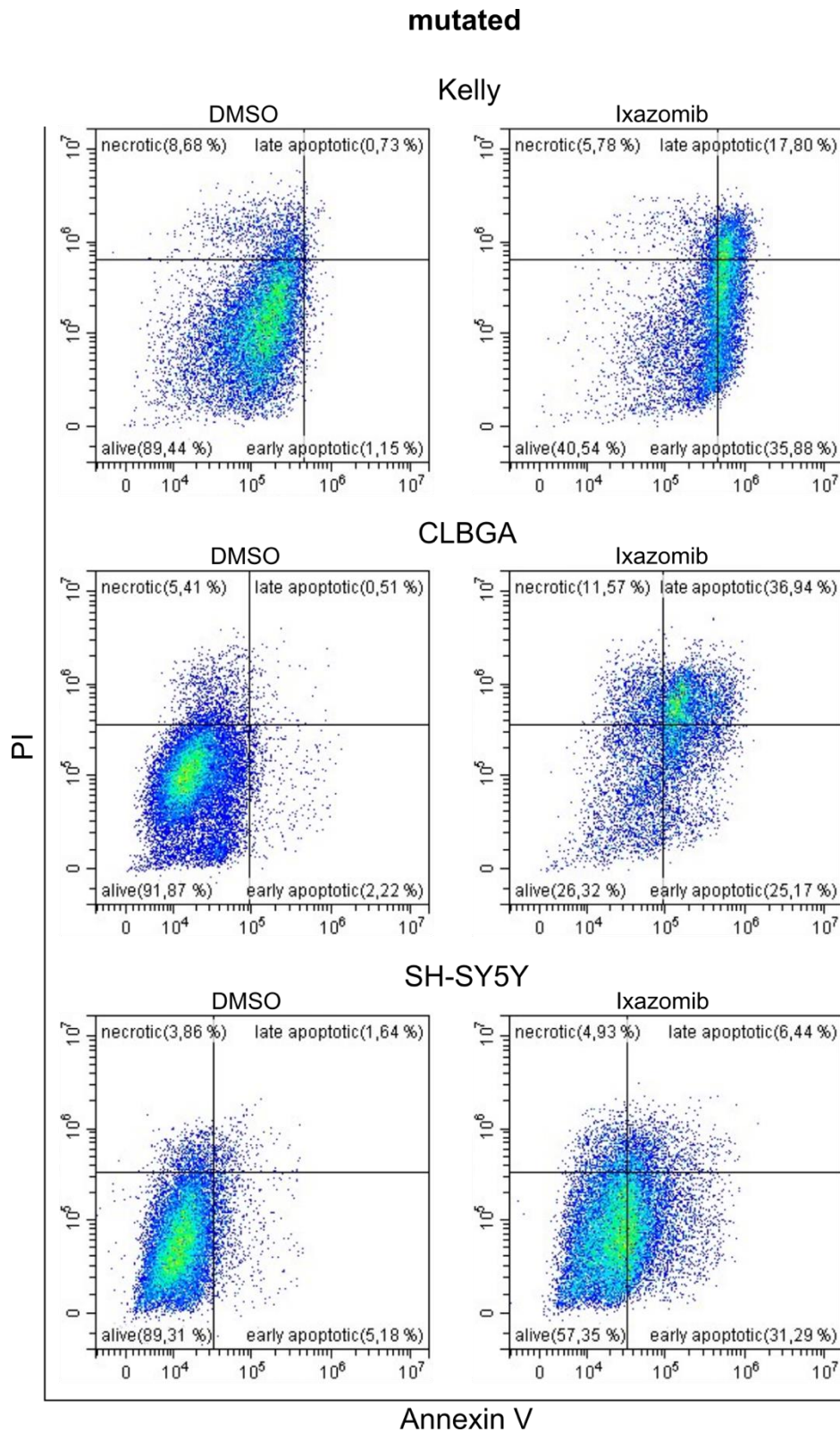


**Figure 5: Increased apoptosis in *ALK* mutated (mut) neuroblastoma (NB) cell lines after ixazomib treatment.** To assess ixazomib-induced apoptosis, NB cell lines were treated with ixazomib (25 nM Kelly cells; 50 nM all other cells) or DMSO as a negative control for 72 h. Thereafter, cells were stained with FITC Annexin V and propidium iodide (PI) and analyzed using flow cytometry. Shown are representative flow cytometry plots. The assay was performed once.

Additionally, an up to 2.4-fold higher caspase 3/7 activity was detected upon ixazomib treatment in *ALK* mut NB cell lines (Figure 6, B). SK-N-FI cells (*ALK* wt) also had a significant 1.35-fold increase in caspase 3/7 activity after ixazomib treatment (Figure 6, A) as well as the highest fraction of apoptotic cells of *ALK* wt NB cells in the Annexin V staining assay which matches the results of the cell viability assay (3.1.1). The results of both experiments indicate a higher apoptosis activity in ixazomib treated *ALK* mut cell lines.

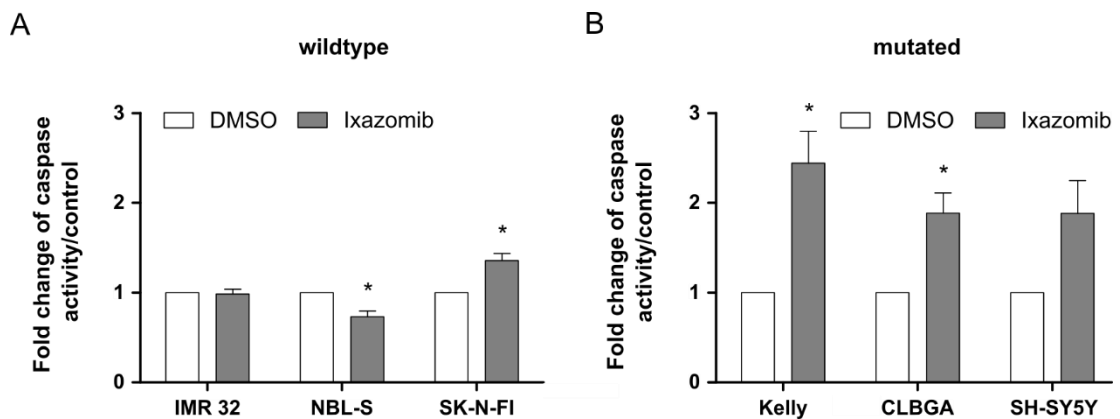


**Figure 6: Ixazomib-dependent induction of caspase 3/7 in *ALK* mutated (mut) neuroblastoma (NB) cells.** To detect caspase 3/7 activity in apoptotic cells, cell lines were treated with ixazomib or DMSO as a negative control. The Caspase-Glo® 3/7 Assay was performed according to the manufacturer's protocol. Luminescence was measured using Spark 10M Microplate Reader. (A, B) Bar graphs represent the fold change of caspase 3/7 activity in ixazomib treated cells compared to the control. Values shown represent mean ± SEM of five independent replicates. \*p<0.05; \*\*p<0.01; \*\*\*p<0.001 (student's t-test).

### 3.1.3 *ALK* mutated neuroblastoma cell lines show more DNA damage upon ixazomib treatment compared to *ALK* wildtype cell lines

For further examination of the possible mechanism of ixazomib-induced apoptosis, an immunofluorescence assay with  $\gamma$ H2A.X was performed to detect DNA double strand breaks.  $\gamma$ H2A.X positive cells were detected in both *ALK* mut and *ALK* wt NB cell lines after ixazomib treatment. On the representative immunofluorescence images, higher effects in *ALK* mut NB cells were noticeable (Figure 7, A). Calculated against the DMSO control, differences were only significant for one of the *ALK* mut cell lines, while two of the *ALK* wt cell lines showed significant differences as well (Figure 7, B, C). Therefore, the amount of DNA damage in *ALK* mut NB cells was also statistically calculated against the amount of DNA damage in *ALK* wt NB cells. For this, pairs were selected based on similar mutation status since some of the cell lines have additional mutations

and these are not equal in all cell lines (Figure 1). This revealed a significant higher amount of DNA damage in *ALK* mut NB cell lines (Figure 7, D). These data indicate that DNA damage plays a role in the mechanism of action of ixazomib.

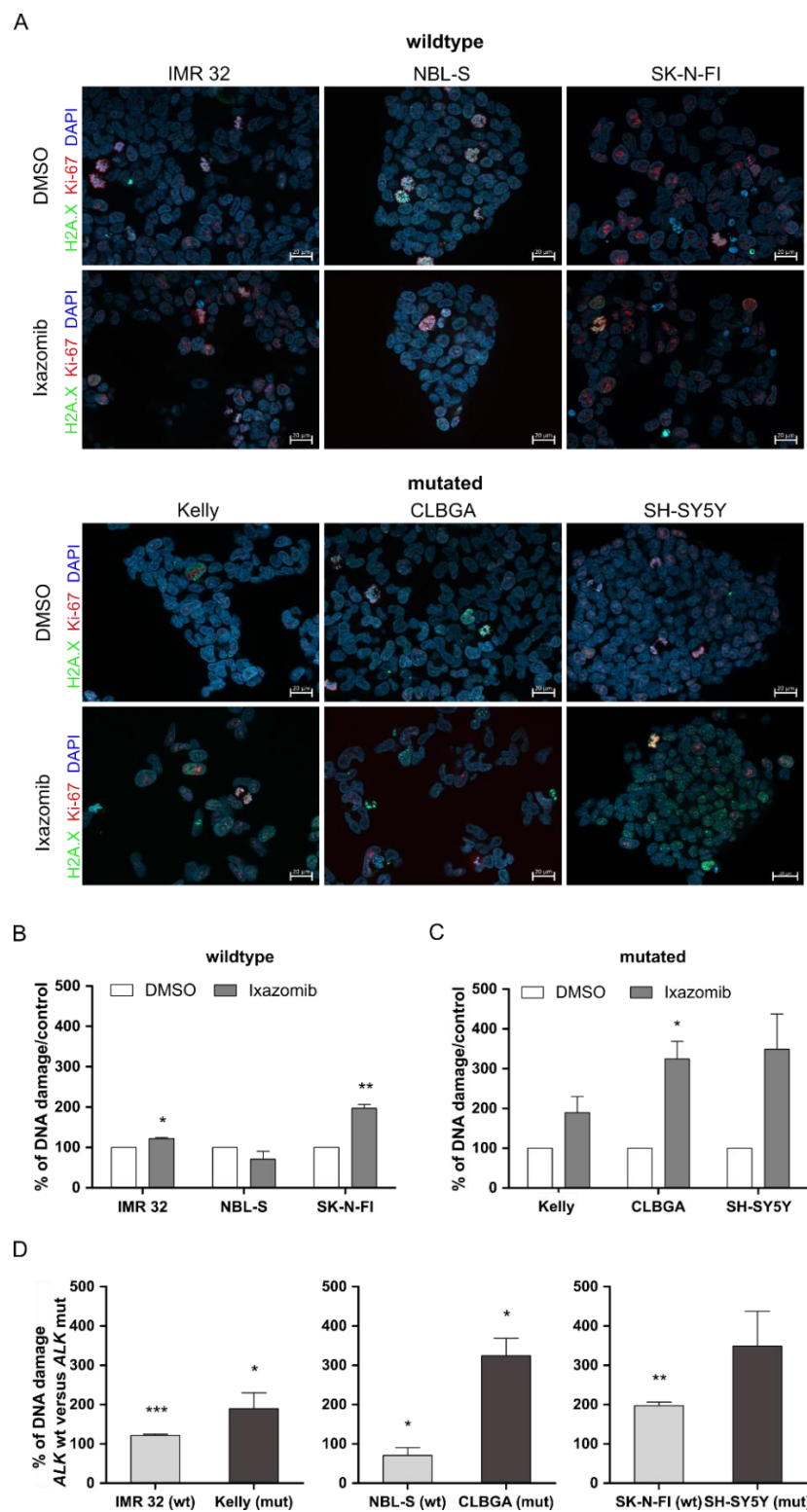


**Figure 7: Ixazomib-induced DNA damage in *ALK* mutated (mut) neuroblastoma (NB) cells.** Ixazomib and DMSO treated cells were incubated overnight with the DNA damage marker  $\gamma$ H2A.X antibody (green) and the proliferation marker Ki-67 antibody (red). Thereafter, cells were fixed and  $\gamma$ H2A.X and Ki-67 were detected using anti-rb Alexa 594 and anti-ms Alexa 488 secondary antibodies. Cells were counterstained with 4',6-diamidino-2-phenylindole (DAPI, blue). Shown

are representative immunofluorescence images (A). The number of  $\gamma$ H2A.X labeled cells relative to DAPI-labeled cells was determined and calculated against the DMSO control and is depicted in B (*ALK* wt) and C (*ALK* mut).  $\gamma$ H2A.X labeled cells after ixazomib treatment of *ALK* wt and mut cells were calculated against each other (D). Values shown represent mean  $\pm$ SEM of at least three replicates. \* $p < 0.05$ ; \*\* $p < 0.01$ ; \*\*\* $p < 0.001$  (student's t-test). The scale bar corresponds to 20  $\mu$ m. Images were taken using a 40x objective.

### 3.2 Possible ixazomib targets in *ALK* mutated neuroblastoma cell lines

In order to elucidate the biological mechanism responsible for the anti-tumoral effect following ixazomib treatment, processed RNA sequencing data for GSE89413 was downloaded from R2 data portal (<https://hgserver1.amc.nl/cgi-bin/r2/main.cgi>). Genes were considered significant if they had a p value  $< 0.05$  and a fold change  $\pm 2$ , for a total of 60 differentially expressed genes. IPA revealed that NF- $\kappa$ B is predicted to be upregulated in *ALK* mut NB cells (Figure 8). Samples with known *ALK* status and available in the Remke laboratory were further investigated regarding the possible interrelation between *ALK* activity, ixazomib treatment and the NF- $\kappa$ B complex.

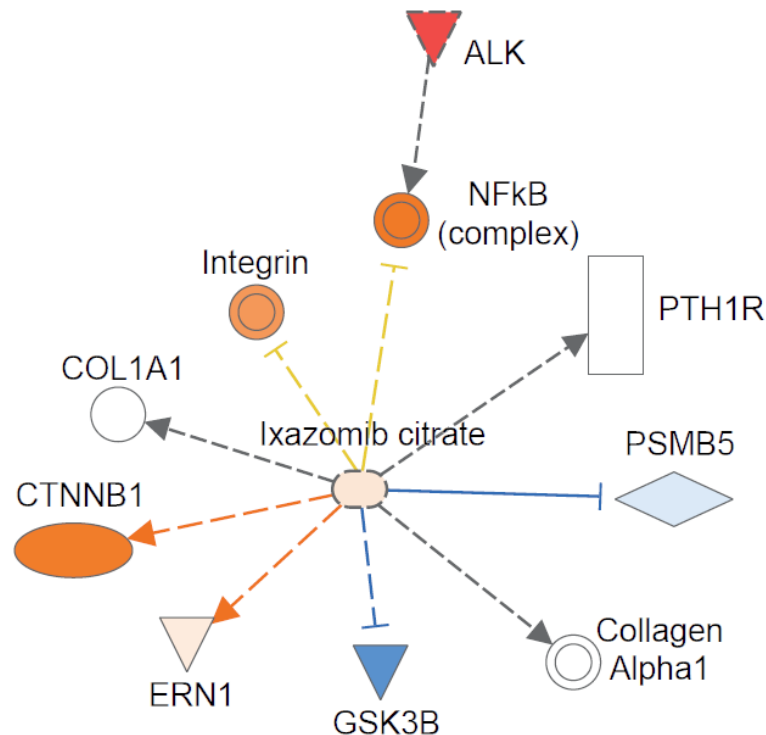


**Figure 8: NF- $\kappa$ B is predicted to be upregulated in *ALK* mutated (mut) neuroblastoma (NB) cells.** Ingenuity pathway analysis (IPA, Qiagen) was conducted using genes with significant differential expression. The significance cut-off for IPA was set to  $p \leq 0.05$  and z score of  $\pm 1.5$ . *ALK* mut NB cells were compared to *ALK* wildtype (wt) NB cell lines. Red indicates that *ALK* is highly expressed in *ALK* mut NB cells. Orange is predicted to be upregulated in *ALK* mut NB. Blue is predicted to be downregulated in *ALK* mut NB. Yellow is predicted to be the opposite direction in *ALK* mut NB.

### 3.3 Validation of NF- $\kappa$ B involvement in the molecular mechanisms of ixazomib in the treatment of *ALK* mutated neuroblastoma on mRNA and protein levels

Given the upregulated expression of *NF- $\kappa$ B* in *ALK* mut NB cells, the expression level of different genes involved in the NF- $\kappa$ B pathway, including *FOS*, *IKBKB*, *NF- $\kappa$ B1*, *NF- $\kappa$ B2*, *RELA*, *RELB*, *RPL13* and *TGM2* were examined after ixazomib treatment. For all tested genes except *NF- $\kappa$ B2* the results were not significant and are therefore not shown. Quantitative real-time PCR revealed a trend for higher *NF- $\kappa$ B2* gene expression in the *ALK* mut cell lines Kelly and CLBGA. The *ALK* mut cell line SH-SY5Y showed a significantly higher expression level of *NF- $\kappa$ B2* gene (Figure 9, B).

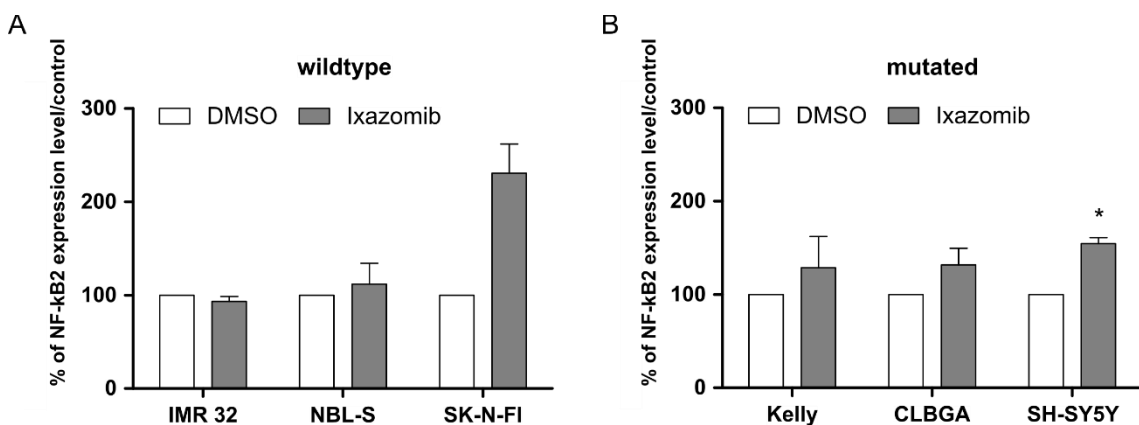


**Figure 9: Ixazomib significantly induced *NF- $\kappa$ B2* expression in SH-SY5Y cells.** Quantitative real-time PCR revealed a higher *nuclear factor kappa B subunit 2* (*NF- $\kappa$ B2*) expression in *ALK* mutated SH-SY5Y cells following ixazomib treatment (B). In all other cell lines, no significant effects were observed (A, B). mRNA expression was normalized to the housekeeping genes *glyceraldehyde-3-phosphate dehydrogenase* (*GAPDH*), *peptidylprolyl isomerase A* (*PPIA*), *glucuronidase beta* (*GUSB*) and *actin beta* (*ACTB*) and calculated relative to the DMSO control. Values shown represent mean  $\pm$ SEM of three independent replicates. \* $p < 0.05$  (students t-test).

Next to the mRNA expression level, also the protein expression level and activity of several proteins involved in the NF- $\kappa$ B-pathway, including IKK $\alpha$ , IKK $\beta$ , I $\kappa$ B $\alpha$  and NF- $\kappa$ B, was investigated by Western blot in ixazomib treated NB cell lines. Notably, an increase in the phosphorylation of NF- $\kappa$ B activation was detected in *ALK* mut NB cell lines investigated, while the endogenous expression of NF- $\kappa$ B was only increased in the *ALK* mut cell line SH-SY5Y (Figure 10 A, B, C). GAPDH served as loading control. Protein expression after ixazomib and DMSO treatment was calculated relative to the loading control. In the *ALK* wt NB cell lines p-NF- $\kappa$ B and NF- $\kappa$ B expression seem to be reduced or stay equal upon

ixazomib treatment. For the other proteins, no difference in expression or activity was observed upon ixazomib treatment, neither in *ALK* mut nor in *ALK* wt NB cell lines (data not shown).

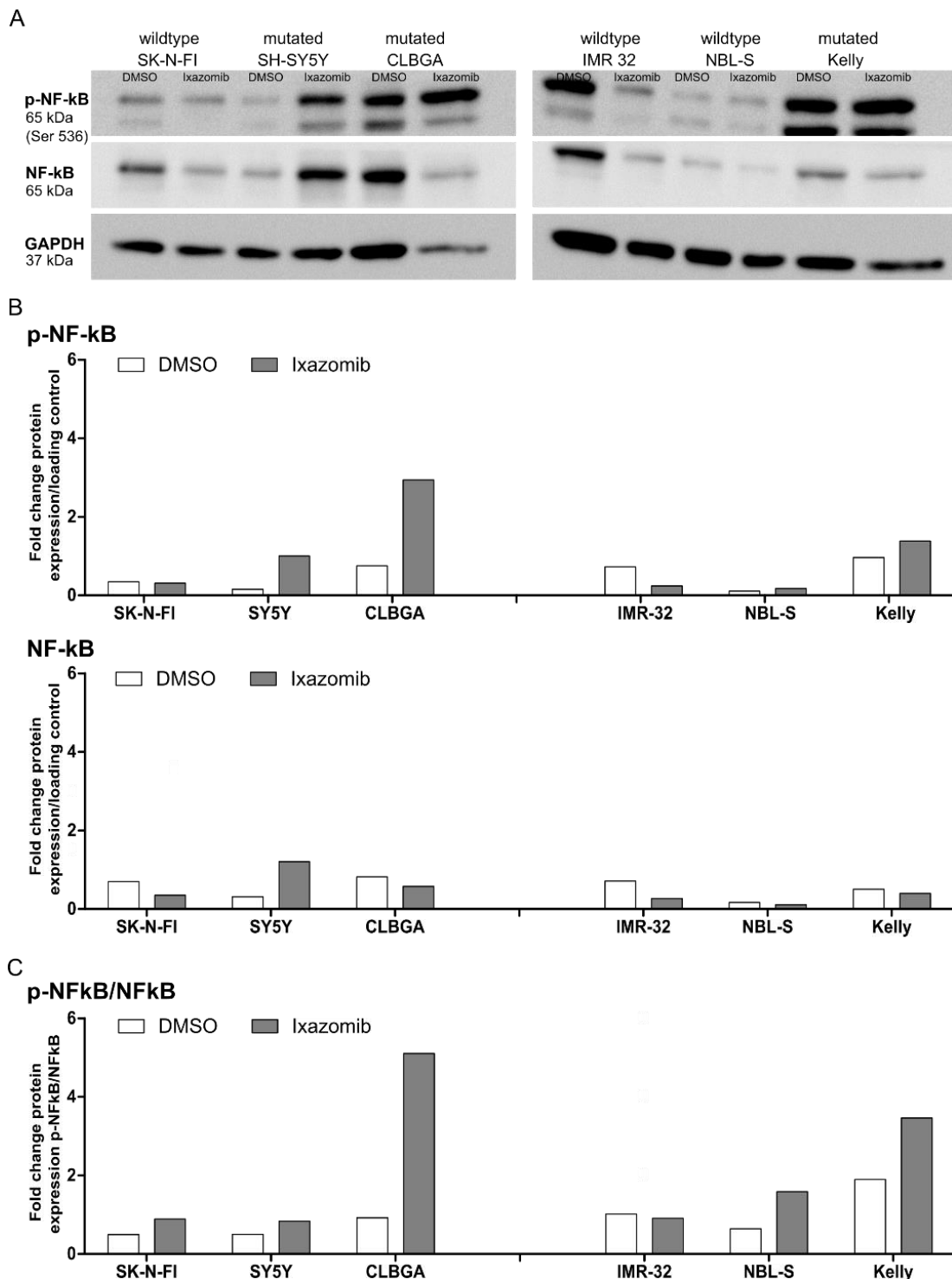


**Figure 10: Ixazomib-induced p-NF- $\kappa$ B activity in *ALK* mutated neuroblastoma cells.** (A) Representative Western blots for phosphorylated nuclear factor kappa B (p-NF- $\kappa$ B), nuclear factor kappa B (NF- $\kappa$ B) and glyceraldehyde 3-phosphate dehydrogenase (GAPDH) as a loading control following treatment with ixazomib and DMSO as a negative control. Protein expression after ixazomib and DMSO treatment was calculated relative to the loading control (B). Protein expression of p-NF- $\kappa$ B in relation to protein expression of NF- $\kappa$ B after ixazomib and DMSO treatment (C). Values and images shown represent one replicate.

## 4 Discussion

The aim of this thesis was a detailed analysis of the therapeutic effects of the relatively new proteasome inhibitor ixazomib in the treatment of NB in relation to the *ALK* mutational status. It was demonstrated that ixazomib leads to decreased cell proliferation and increased DNA damage and apoptosis especially in *ALK* mut NB cell lines. Further investigations on NF- $\kappa$ B function revealed possible *ALK*-dependent alteration of NF- $\kappa$ B activity.

### 4.1 Importance of novel therapeutic strategies for neuroblastoma

For patients with high-risk NB, which is detected in about 60% of cases, a broad range of therapeutic options have been developed over the past decades [8, 58, 59]. Nevertheless, the survival rate remains only about 50% [60, 61]. In addition, the likelihood of developing resistance to the commonly used chemotherapeutic agents increases with each relapse [61]. In the end, this leads to increasing difficulties in finding a suitable therapy for patients at relapse. This is reflected in the five-year overall survival for patients with relapsing NB, which is reported to be 20% only [62]. Another point to consider is that patients who survive therapy often suffer from long-term, eventually life-threatening complications after therapy [63]. Outcomes could be improved by intensified therapy regimens. However, this would also increase the probability of long-term complications, and survival rates may not be substantially improved [39]. Therefore, new therapy options are needed. In 8-10% of all NBs, *ALK* mutations are found and seem to be an appealing target for new therapy strategies [22-24].

After ixazomib emerged as a promising inhibitor for *ALK* mut NB in a high-throughput drug screening, its efficacy was tested in this thesis. Among the most frequently described effects of ixazomib and other proteasome inhibitors on different types of cancers, including NB, are reduced proliferation and viability and increased apoptosis [43, 44, 53, 64-67]. In this study, this was also validated in NB cell line models. Notably, the effect on *ALK* mut NB cells was significantly stronger compared to *ALK* wt NB cells.

## 4.2 Additional mutations influencing the effect of ixazomib in neuroblastoma cell lines

Some of the cell lines investigated in this thesis carry additional mutations apart from *ALK* (e.g., SK-N-FI, SH-SY5Y (Table 1)), which may have an impact on the therapeutic effect of ixazomib.

Even though SK-N-FI is an *ALK* wt NB cell line, ixazomib had a stronger effect on the cell line than on the other *ALK* wt NB cell lines, IMR 32 and NBL-S. SK-N-FI has a loss of function mutation in *TP53* [68]. P53, one of the most important cell cycle, DNA repair and apoptosis regulating proteins, is frequently altered in human tumors [69]. In NB, *TP53* mutations are rarely found at diagnosis and normally occur later in the disease course in relapsed tumors [69]. Blanco-Luquin et al. performed an *in vitro* study comparing the effect of different chemotherapeutic drugs on *TP53* mut and *TP53* wt cell lines. They concluded that the *TP53*-mut SK-N-FI cells respond better to some of these drugs [68]. In *ALK* rearranged NSCLC with *TP53* mutation the combined therapy of a proteasome inhibitor and the *ALK* inhibitor alectinib seemed to be more effective than monotherapy with alectinib [70]. This might explain why ixazomib has a stronger effect on SK-N-FI cells than on the other *ALK* wt cell lines IMR 32 and NBL-S.

Furthermore, a higher amount of DNA damage in ixazomib treated *ALK* mut NB cells compared to *ALK* wt NB cells was detected. Proteasome inhibition leads to apoptosis through caspase-9 activation and increasing levels of NOXA [71]. NOXA, a pro-apoptotic member of the Bcl-2 family, is a mediator of *TP53*-dependent detection of DNA damage and consequently apoptosis [72]. The proteasome usually degrades NOXA rapidly [73]. NOXA expression can be induced by proteasome inhibitors independently of *TP53*, leading to DNA damage and apoptosis by an *TP53*-independent pathway [67]. In summary, it is suspected that the ixazomib treatment leads to apoptosis by *TP53*-dependent as well as -independent mechanisms and may therefore be influenced by the *TP53* status of the cells.

On SH-SY5Y, an *ALK* mut NB cell line, ixazomib seems to be less effective than on the other *ALK* mut cell lines, Kelly and CLBGA. One mutation that distinguishes the cell line SH-SY5Y from the other two cell lines is the *TERT*

promoter mutation C228T in SH-SY5Y cells [55]. *TERT* mutations belong to most common point mutations in different tumor types [74]. *TERT* rearrangements occur only in high-risk NB and seem to be correlated with a particular poor outcome [54]. Furthermore, *TERT* promoter mutations are often associated with aggressive disease even though they are probably not relevant for NB pathogenesis [55]. Drug resistance caused by *TERT* mutations is not described in literature. Therefore, it remains questionable whether this mutation is the reason for the less strong effect of ixazomib on SH-SY5Y cells. Other differences between the *ALK* mut NB cell lines that would explain the poorer response of SH-SY5Y to ixazomib treatment still need to be elucidated.

#### **4.3 NF- $\kappa$ B as possible target for ixazomib in neuroblastoma cell lines**

The downstream events after inhibition of the proteasome and thus the exact mechanism of action of proteasome inhibitors is not yet entirely clear [44]. To investigate possible molecular mechanisms involved in the increased therapeutic effect of ixazomib in NB cells lines with *ALK* mutations, IPA was performed on public available data. The analysis predicted that NF- $\kappa$ B signaling appears to be upregulated in *ALK* mut NB cells after ixazomib treatment. Therefore, NF- $\kappa$ B expression and activity in *ALK* mut NB cells was investigated as possible molecular target for the higher sensitivity of the cells towards ixazomib.

It is known that proteasome inhibitors influence the NF- $\kappa$ B pathway and its downstream events [43, 75]. NF- $\kappa$ B is a specific transcription factor that is particularly important in the regulation of immune response, cell proliferation and apoptosis [76]. In tumor cells, dysregulation of NF- $\kappa$ B can occur, resulting in permanent NF- $\kappa$ B activation. Among others, NF- $\kappa$ B regulates genes involved in cell cycle control, adhesion, migration and apoptosis, processes that promote carcinogenesis when regulation is abrogated [77]. The proteasome is important for NF- $\kappa$ B activation [75]. The active form of NF- $\kappa$ B (p50 and p52) is generated by proteolysis [77]. Furthermore, NF- $\kappa$ B is regulated through inhibitory proteins, I $\kappa$ Bs, which are degraded through the proteasome. I $\kappa$ Bs bind NF- $\kappa$ B and thereby prevent its nuclear uptake [76, 78]. The complete degradation of the inhibiting proteins is necessary for the translocation of NF- $\kappa$ B into the nucleus [75]. Proteasome inhibition indirectly leads to lower activation of NF- $\kappa$ B.

NF- $\kappa$ B is composed of a family of transcription factors that includes the following five genes: *NF- $\kappa$ B1*, *NF- $\kappa$ B2*, *RELA*, *RELB* and *c-Rel* [77]. In this thesis it was analyzed, if there are differences in the expression levels of these genes and, in addition, *FOS*, *IKBKB*, *TGM 2*, *RPL13*, which all may influence the NF- $\kappa$ B pathway [79, 80] in *ALK* mut NB and *ALK* wt cells after ixazomib treatment. Unfortunately, no significant differences could be observed in the experimental set-up for the investigated parameters. Only slight ixazomib-induced upregulated *NF- $\kappa$ B2* levels in *ALK* mut NB cells were found. Further experiments are needed to understand the *ALK*-dependent interrelation of ixazomib treatment with the NF- $\kappa$ B pathway.

The multi-subunit IKK contains two catalytic subunits, IKK $\alpha$  and IKK $\beta$ , and is responsible for the phosphorylation of I $\kappa$ B. Once phosphorylated, I $\kappa$ B can be degraded by the proteasome resulting in the activation of NF- $\kappa$ B [76, 78]. To evaluate whether the protein activity of proteins from the NF- $\kappa$ B pathway, including IKK $\alpha$ , IKK $\beta$ , I $\kappa$ B $\alpha$  and NF- $\kappa$ B, is different in *ALK* mut NB cells in comparison to *ALK* wt NB cells after ixazomib treatment, protein expression levels were analyzed. It was hypothesized to see higher levels of I $\kappa$ B $\alpha$  after proteasome inhibition, and therefore, lower levels of NF- $\kappa$ B. However, only slightly higher p-NF- $\kappa$ B levels in *ALK* mut NB cells were observed after ixazomib treatment.

These results indicate that *ALK* mutation affects NB cells by upregulating NF- $\kappa$ B but that the altered NF- $\kappa$ B pathway and its downstream events may not be the only mechanism of action for ixazomib treatment in NB cells, and that there must be further molecular alterations induced by *ALK* mutation in NB cells, i.e., other than those affecting the NF- $\kappa$ B pathway.

For instance, blocking of p53 degradation through proteasome inhibition could contribute to tumor suppression [44] and the c-Jun NH<sub>2</sub>terminal kinase (JNK) activation through proteasome inhibition can result in apoptosis [43]. These are just two examples for the different effects of proteasome inhibition at the cellular level. To answer the question which mechanisms play a role in the ixazomib treatment of *ALK* mut NB, further research is needed.

#### **4.4 Development of resistance of *ALK* mutated neuroblastomas to *ALK* inhibitors**

An obvious approach to search for therapeutic options for *ALK* mut NB would be to investigate *ALK* inhibitors. The first generation *ALK* inhibitor crizotinib was FDA approved in 2011 for the treatment of *ALK* mut NSCLC [81]. In 2018, it was first approved for pediatric use in the context of anaplastic large cell non-Hodgkin lymphoma (ALCL). In 2021, it was tested in patients with relapsed or refractory *ALK* mut NB. Unfortunately, the activity seen in this trial was limited [82]. Currently, the third generation *ALK* inhibitor lorlatinib is being evaluated for the therapy of relapsed NB because the most prevalent *ALK* mutation F1174L is resistant to the first generation *ALK* inhibitor crizotinib [23], and development of resistance seems to also be a problem with the second generation inhibitor ceritinib [36, 82-84]. Crizotinib lacks efficacy against most of the *ALK* mutations found in NB, which is another reason for the current evaluation of new *ALK* inhibitors [85].

Taking resistance mechanisms with *ALK* inhibitors into account, research for alternative therapeutic compounds, such as the proteasome inhibitors, seems highly important. Additionally, ixazomib has the advantages of oral availability as well as a limited spectrum of adverse events [51]. These characteristics of ixazomib should also be taken into consideration in the context of finding new therapeutic options for *ALK* mut NB.

#### **4.5 Limitations**

Some of the experiments presented in this thesis were only performed with a limited number of cell lines or were only repeated once. For instance, EdU proliferation assay was performed only with a part of the cell lines. Assays that have been performed only once are crystal violet staining, Annexin-V based FACS and Western blot analysis. All of them need to be repeated at least two times to be quantitatively evaluable.

Nevertheless, the difference in the effect of ixazomib on *ALK* mut cells and *ALK* wt cells was evident for the proliferation assay, the crystal violet staining as well as for the Annexin V-based FACS apoptosis assay, and, therefore, were regarded as important findings. When the results of these experiments were

viewed together in the context of the subsequent experiments, the results are considered as conclusive.

#### **4.6 Conclusion and Outlook**

In conclusion, it was demonstrated that ixazomib is highly effective in the treatment of various NB cell lines with clear relation to a high effectiveness depending on the *ALK* mutational status. The molecular mechanism of action still needs to be elucidated. Furthermore, the results of these experiments in cell culture have to be translated into the *in vivo* setting in animal models and patients. Proteasome inhibition appears as a promising strategy in the course of therapy for patients with NB.

## 5 References

1. Maris, J.M., *Recent advances in neuroblastoma*. N Engl J Med, 2010. **362**(23): p. 2202-11.
2. Qiu, B. and K.K. Matthay, *Advancing therapy for neuroblastoma*. Nat Rev Clin Oncol, 2022. **19**(8): p. 515-533.
3. <https://seer.cancer.gov/>. [cited 2022 25.11.]; Available from: [https://seer.cancer.gov/archive/csr/1975\\_2018/browse\\_csr.php?sectionSEL=2&pageSEL=sect\\_02\\_table.06](https://seer.cancer.gov/archive/csr/1975_2018/browse_csr.php?sectionSEL=2&pageSEL=sect_02_table.06).
4. Brodeur, G.M., *Spontaneous regression of neuroblastoma*. Cell Tissue Res, 2018. **372**(2): p. 277-286.
5. Jin, Q.Y., S.B. Du, and X.J. Yuan, *Exploring the prognosis of neuroblastoma in adolescents and adults: a case series and literature review*. Neoplasma, 2022. **69**(2): p. 464-473.
6. Brodeur, G.M., *Neuroblastoma: biological insights into a clinical enigma*. Nat Rev Cancer, 2003. **3**(3): p. 203-16.
7. Erdmann F, K.P., Grabow D, Spix C, *German Childhood Cancer Registry - Annual Report 2019 (1980-2018)*. Institute of Medical Biostatistics, Epidemiology and Informatics (IMBEI) at the University Medical Center of the Johannes Gutenberg University Mainz. 2020.
8. Simon, T., et al., *2017 GPOH Guidelines for Diagnosis and Treatment of Patients with Neuroblastic Tumors*. Klin Padiatr, 2017. **229**(3): p. 147-167.
9. Maris, J.M., et al., *Neuroblastoma*. Lancet, 2007. **369**(9579): p. 2106-20.
10. Simon, T., *S1-Leitlinie Neuroblastom* 2019.
11. Barco, S., et al., *Urinary homovanillic and vanillylmandelic acid in the diagnosis of neuroblastoma: report from the Italian Cooperative Group for Neuroblastoma*. Clin Biochem, 2014. **47**(9): p. 848-52.
12. Ferraro, S., et al., *Measurement of Serum Neuron-Specific Enolase in Neuroblastoma: Is There a Clinical Role?* Clin Chem, 2020. **66**(5): p. 667-675.
13. Brisse, H.J., et al., *Guidelines for imaging and staging of neuroblastic tumors: consensus report from the International Neuroblastoma Risk Group Project*. Radiology, 2011. **261**(1): p. 243-57.
14. Olivier, P., et al., *Guidelines for radioiodinated MIBG scintigraphy in children*. Eur J Nucl Med Mol Imaging, 2003. **30**(5): p. B45-50.
15. Swift, C.C., et al., *Updates in Diagnosis, Management, and Treatment of Neuroblastoma*. Radiographics, 2018. **38**(2): p. 566-580.
16. Cohn, S.L., et al., *The International Neuroblastoma Risk Group (INRG) classification system: an INRG Task Force report*. J Clin Oncol, 2009. **27**(2): p. 289-97.
17. Westermann, F. and M. Schwab, *Genetic parameters of neuroblastomas*. Cancer Lett, 2002. **184**(2): p. 127-47.
18. Schneiderman, J., et al., *Clinical significance of MYCN amplification and ploidy in favorable-stage neuroblastoma: a report from the Children's Oncology Group*. J Clin Oncol, 2008. **26**(6): p. 913-8.
19. Schleiermacher, G., et al., *Segmental chromosomal alterations have prognostic impact in neuroblastoma: a report from the INRG project*. Br J Cancer, 2012. **107**(8): p. 1418-22.
20. Attiyeh, E.F., et al., *Chromosome 1p and 11q deletions and outcome in neuroblastoma*. N Engl J Med, 2005. **353**(21): p. 2243-53.
21. Pugh, T.J., et al., *The genetic landscape of high-risk neuroblastoma*. Nat Genet, 2013. **45**(3): p. 279-84.
22. Lundberg, K.I., D. Treis, and J.I. Johnsen, *Neuroblastoma Heterogeneity, Plasticity, and Emerging Therapies*. Curr Oncol Rep, 2022. **24**(8): p. 1053-1062.
23. Azarova, A.M., G. Gautam, and R.E. George, *Emerging importance of ALK in neuroblastoma*. Semin Cancer Biol, 2011. **21**(4): p. 267-75.
24. O'Donohue, T., et al., *Differential Impact of ALK Mutations in Neuroblastoma*. JCO Precis Oncol, 2021. **5**.
25. Mosse, Y.P., et al., *Identification of ALK as a major familial neuroblastoma predisposition gene*. Nature, 2008. **455**(7215): p. 930-5.
26. Mosse, Y.P., et al., *Germline PHOX2B mutation in hereditary neuroblastoma*. Am J Hum Genet, 2004. **75**(4): p. 727-30.

27. Matthay, K.K., et al., *Long-term results for children with high-risk neuroblastoma treated on a randomized trial of myeloablative therapy followed by 13-cis-retinoic acid: a children's oncology group study*. *J Clin Oncol*, 2009. **27**(7): p. 1007-13.
28. DuBois, S.G. and K.K. Matthay, *Radiolabeled metaiodobenzylguanidine for the treatment of neuroblastoma*. *Nucl Med Biol*, 2008. **35 Suppl 1**: p. S35-48.
29. Matthay, K.K., et al., *Dose escalation study of no-carrier-added 131I-metaiodobenzylguanidine for relapsed or refractory neuroblastoma: new approaches to neuroblastoma therapy consortium trial*. *J Nucl Med*, 2012. **53**(7): p. 1155-63.
30. Ducray, S.P., et al., *The Transcriptional Roles of ALK Fusion Proteins in Tumorigenesis*. *Cancers (Basel)*, 2019. **11**(8).
31. Iwahara, T., et al., *Molecular characterization of ALK, a receptor tyrosine kinase expressed specifically in the nervous system*. *Oncogene*, 1997. **14**(4): p. 439-49.
32. Morris, S.W., et al., *Fusion of a kinase gene, ALK, to a nucleolar protein gene, NPM, in non-Hodgkin's lymphoma*. *Science*, 1994. **263**(5151): p. 1281-4.
33. Osajima-Hakomori, Y., et al., *Biological role of anaplastic lymphoma kinase in neuroblastoma*. *Am J Pathol*, 2005. **167**(1): p. 213-22.
34. Lee, C.C., et al., *Crystal structure of the ALK (anaplastic lymphoma kinase) catalytic domain*. *Biochem J*, 2010. **430**(3): p. 425-37.
35. Bresler, S.C., et al., *ALK mutations confer differential oncogenic activation and sensitivity to ALK inhibition therapy in neuroblastoma*. *Cancer Cell*, 2014. **26**(5): p. 682-94.
36. Mosse, Y.P., et al., *Safety and activity of crizotinib for paediatric patients with refractory solid tumours or anaplastic large-cell lymphoma: a Children's Oncology Group phase 1 consortium study*. *Lancet Oncol*, 2013. **14**(6): p. 472-80.
37. Caren, H., et al., *High incidence of DNA mutations and gene amplifications of the ALK gene in advanced sporadic neuroblastoma tumours*. *Biochem J*, 2008. **416**(2): p. 153-9.
38. Lee, J.W., et al., *ALK Protein Expression Is Related to Neuroblastoma Aggressiveness But Is Not Independent Prognostic Factor*. *Cancer Res Treat*, 2018. **50**(2): p. 495-505.
39. Carpenter, E.L. and Y.P. Mosse, *Targeting ALK in neuroblastoma--preclinical and clinical advancements*. *Nat Rev Clin Oncol*, 2012. **9**(7): p. 391-9.
40. Rosswog, C., et al., *Genomic ALK alterations in primary and relapsed neuroblastoma*. *Br J Cancer*, 2023. **128**(8): p. 1559-1571.
41. George, R.E., et al., *Activating mutations in ALK provide a therapeutic target in neuroblastoma*. *Nature*, 2008. **455**(7215): p. 975-8.
42. Schulte, J.H., et al., *High ALK receptor tyrosine kinase expression supersedes ALK mutation as a determining factor of an unfavorable phenotype in primary neuroblastoma*. *Clin Cancer Res*, 2011. **17**(15): p. 5082-92.
43. Nunes, A.T. and C.M. Annunziata, *Proteasome inhibitors: structure and function*. *Semin Oncol*, 2017. **44**(6): p. 377-380.
44. Fricker, L.D., *Proteasome Inhibitor Drugs*. *Annu Rev Pharmacol Toxicol*, 2020. **60**: p. 457-476.
45. Park, J.E., et al., *Next-generation proteasome inhibitors for cancer therapy*. *Transl Res*, 2018. **198**: p. 1-16.
46. <https://www.ema.europa.eu/Fachinformation/Bortezomib> [cited 2022 25.11.]; Available from: [https://www.ema.europa.eu/en/documents/product-information/velcade-epar-product-information\\_de.pdf](https://www.ema.europa.eu/en/documents/product-information/velcade-epar-product-information_de.pdf).
47. <https://www.ema.europa.eu/Fachinformation/Ixazomib>. [cited 2022 25.11.]; Available from: [https://www.ema.europa.eu/en/documents/product-information/ninlaro-epar-product-information\\_de.pdf](https://www.ema.europa.eu/en/documents/product-information/ninlaro-epar-product-information_de.pdf).
48. <https://www.ema.europa.eu/Fachinformation/Carfilzomib> [cited 2022 25.11.]; Available from: [https://www.ema.europa.eu/en/documents/product-information/kyprolis-epar-product-information\\_de.pdf](https://www.ema.europa.eu/en/documents/product-information/kyprolis-epar-product-information_de.pdf).
49. <https://clinicaltrials.gov>. [cited 2022 25.11.]; Available from: <https://clinicaltrials.gov/ct2/results?cond=&term=Bortezomib&cntry=&state=&city=&dist=>  
<https://clinicaltrials.gov/ct2/results?cond=&term=Ixazomib&cntry=&state=&city=&dist=>
50. Gandolfi, S., et al., *The proteasome and proteasome inhibitors in multiple myeloma*. *Cancer Metastasis Rev*, 2017. **36**(4): p. 561-584.

51. Manasanch, E.E. and R.Z. Orlowski, *Proteasome inhibitors in cancer therapy*. *Nat Rev Clin Oncol*, 2017. **14**(7): p. 417-433.
52. Roeten, M.S.F., J. Cloos, and G. Jansen, *Positioning of proteasome inhibitors in therapy of solid malignancies*. *Cancer Chemother Pharmacol*, 2018. **81**(2): p. 227-243.
53. Li, H., et al., *Novel proteasome inhibitor ixazomib sensitizes neuroblastoma cells to doxorubicin treatment*. *Sci Rep*, 2016. **6**: p. 34397.
54. Peifer, M., et al., *Telomerase activation by genomic rearrangements in high-risk neuroblastoma*. *Nature*, 2015. **526**(7575): p. 700-4.
55. Lindner, S., et al., *Absence of telomerase reverse transcriptase promoter mutations in neuroblastoma*. *Biomed Rep*, 2015. **3**(4): p. 443-446.
56. Bradford, M.M., *A rapid and sensitive method for the quantitation of microgram quantities of protein utilizing the principle of protein-dye binding*. *Anal Biochem*, 1976. **72**: p. 248-54.
57. Muz, B., et al., *Spotlight on ixazomib: potential in the treatment of multiple myeloma*. *Drug Des Devel Ther*, 2016. **10**: p. 217-26.
58. Zafar, A., et al., *Molecular targeting therapies for neuroblastoma: Progress and challenges*. *Med Res Rev*, 2021. **41**(2): p. 961-1021.
59. Kholodenko, I.V., et al., *Neuroblastoma Origin and Therapeutic Targets for Immunotherapy*. *J Immunol Res*, 2018. **2018**: p. 7394268.
60. Matthay, K.K., et al., *Neuroblastoma*. *Nat Rev Dis Primers*, 2016. **2**: p. 16078.
61. Whittle, S.B., et al., *Overview and recent advances in the treatment of neuroblastoma*. *Expert Rev Anticancer Ther*, 2017. **17**(4): p. 369-386.
62. London, W.B., et al., *Clinical and biologic features predictive of survival after relapse of neuroblastoma: a report from the International Neuroblastoma Risk Group project*. *J Clin Oncol*, 2011. **29**(24): p. 3286-92.
63. Smith, M.A., et al., *Outcomes for children and adolescents with cancer: challenges for the twenty-first century*. *J Clin Oncol*, 2010. **28**(15): p. 2625-34.
64. Wang, Q., et al., *Ixazomib inhibits myeloma cell proliferation by targeting UBE2K*. *Biochem Biophys Res Commun*, 2021. **549**: p. 1-7.
65. Wang, T., et al., *Ixazomib Induces Apoptosis and Suppresses Proliferation in Esophageal Squamous Cell Carcinoma through Activation of the c-Myc/NOXA Pathway*. *J Pharmacol Exp Ther*, 2022. **380**(1): p. 15-25.
66. Fan, Q. and B. Liu, *Identification of the anticancer effects of a novel proteasome inhibitor, ixazomib, on colorectal cancer using a combined method of microarray and bioinformatics analysis*. *Oncotargets Ther*, 2017. **10**: p. 3591-3606.
67. Pandit, B. and A.L. Gartel, *Proteasome inhibitors induce p53-independent apoptosis in human cancer cells*. *Am J Pathol*, 2011. **178**(1): p. 355-60.
68. Blanco-Luquin, I., et al., *In Vitro Assessment of the Role of p53 on Chemotherapy Treatments in Neuroblastoma Cell Lines*. *Pharmaceuticals (Basel)*, 2021. **14**(11).
69. Goldschneider, D., et al., *Expression of C-terminal deleted p53 isoforms in neuroblastoma*. *Nucleic Acids Res*, 2006. **34**(19): p. 5603-12.
70. Tanimoto, A., et al., *Proteasome Inhibition Overcomes ALK-TKI Resistance in ALK-Rearranged/TP53-Mutant NSCLC via Noxa Expression*. *Clin Cancer Res*, 2021. **27**(5): p. 1410-1420.
71. Qin, J.Z., et al., *Proteasome inhibitors trigger NOXA-mediated apoptosis in melanoma and myeloma cells*. *Cancer Res*, 2005. **65**(14): p. 6282-93.
72. Oda, E., et al., *Noxa, a BH3-only member of the Bcl-2 family and candidate mediator of p53-induced apoptosis*. *Science*, 2000. **288**(5468): p. 1053-8.
73. Ploner, C., R. Kofler, and A. Villunger, *Noxa: at the tip of the balance between life and death*. *Oncogene*, 2008. **27 Suppl 1**: p. S84-92.
74. Bell, R.J., et al., *Understanding TERT Promoter Mutations: A Common Path to Immortality*. *Mol Cancer Res*, 2016. **14**(4): p. 315-23.
75. Palombella, V.J., et al., *The ubiquitin-proteasome pathway is required for processing the NF-kappa B1 precursor protein and the activation of NF-kappa B*. *Cell*, 1994. **78**(5): p. 773-85.
76. Karin, M. and Y. Ben-Neriah, *Phosphorylation meets ubiquitination: the control of NF-[kappa]B activity*. *Annu Rev Immunol*, 2000. **18**: p. 621-63.
77. Dolcet, X., et al., *NF-kB in development and progression of human cancer*. *Virchows Arch*, 2005. **446**(5): p. 475-82.

78. Mitchell, S., J. Vargas, and A. Hoffmann, *Signaling via the NFkappaB system*. Wiley Interdiscip Rev Syst Biol Med, 2016. **8**(3): p. 227-41.
79. Malkomes, P., et al., *Transglutaminase 2 promotes tumorigenicity of colon cancer cells by inactivation of the tumor suppressor p53*. Oncogene, 2021. **40**(25): p. 4352-4367.
80. Lee, S., et al., *IKBKB siRNA-Encapsulated Poly (Lactic-co-Glycolic Acid) Nanoparticles Diminish Neuropathic Pain by Inhibiting Microglial Activation*. Int J Mol Sci, 2021. **22**(11).
81. <https://ema.europa.eu> Fachinformation Crizotinib [cited 2022 25.11.]; Available from: [https://www.ema.europa.eu/en/documents/product-information/xalkori-epar-product-information\\_de.pdf](https://www.ema.europa.eu/en/documents/product-information/xalkori-epar-product-information_de.pdf).
82. Foster, J.H., et al., *Activity of Crizotinib in Patients with ALK-Aberrant Relapsed/Refractory Neuroblastoma: A Children's Oncology Group Study (ADVL0912)*. Clin Cancer Res, 2021. **27**(13): p. 3543-3548.
83. Berlak, M., et al., *Mutations in ALK signaling pathways conferring resistance to ALK inhibitor treatment lead to collateral vulnerabilities in neuroblastoma cells*. Mol Cancer, 2022. **21**(1): p. 126.
84. Fischer, M., et al., *Ceritinib in paediatric patients with anaplastic lymphoma kinase-positive malignancies: an open-label, multicentre, phase 1, dose-escalation and dose-expansion study*. Lancet Oncol, 2021. **22**(12): p. 1764-1776.
85. Schulte, J.H. and A. Eggert, *ALK Inhibitors in Neuroblastoma: A Sprint from Bench to Bedside*. Clin Cancer Res, 2021. **27**(13): p. 3507-3509.

## Acknowledgement

I would like to thank my supervisor, Prof. Dr. Guido Reifenberger, for giving me the opportunity to work on this interesting project.

Furthermore, I would like to thank PD Dr. Sujal Ghosh for evaluating my thesis as a second supervisor.

I would like to thank the Forschungskommission of the Medical Faculty, Heinrich Heine University Düsseldorf, for financial support.

I would like to particularly thank Prof. Dr. Marc Remke for giving me the possibility to work on this project in his laboratory and his support throughout the years.

I would like to thank all members of the KMT lab for the great working atmosphere.

A big thank you to all current and former members of AG Remke. I had an amazing time at the lab and even though we had to miss out on a lot of get togethers during my time in the lab due to COVID-19. I am really grateful to get to know all of you and to have been working together with you.

A special thanks goes to Jasmin. Thank you for helping me through the whole process of working on and writing this thesis. This work would not have been possible without your support. Thank you as well for proofreading this thesis.

Another big thank you goes to Lena for proofreading this thesis, always helping me out, teaching me a lot and a lot of good times in the lab.

Sarah, Frauke, Nan and Daniel, thank you for all the support and helping out in so many instances. Especially, I would like to thank Daniel for helping me with the IPA for this thesis and proofreading.

Felix, Taya, Fiona and Stefan thank you for the great time together in the lab. It would not have been the same without you.

Also, I would like to thank all my friends that accompanied me during my time in Düsseldorf. Thank you for all the good times and distractions outside the hospital and the lab.

The biggest thank you goes to my family and to Nils. Thank you for always supporting me, having an open ear, being there and helping out with any problems. I could not have done this without you.